(12) INTERNATIONAL APPLICATION PUBLISHED UNDER THE PATENT COOPERATION TREATY (PCT)

(19) World Intellectual Property Organization
International Bureau

(43) International Publication Date
14 May 2015 (14.05.2015)

WIPO | PCT

(10) International Publication Number
WO 2015/069817 A1

(51) International Patent Classification:
E21B 43/26 (2006.01) *E21B 43/247* (2006.01)

(21) International Application Number:
PCT/US2014/064205

(22) International Filing Date:
6 November 2014 (06.11.2014)

(25) Filing Language: English

(26) Publication Language: English

(30) Priority Data:
61/900,479 6 November 2013 (06.11.2013) US

(71) Applicant *(for CA only)*: **SCHLUMBERGER CANADA LIMITED** [CA/CA]; 125 - 9 Avenue SE, Calgary, Alberta T2G 0P6 (CA).

(71) Applicant *(for FR only)*: **SERVICES PETROLIERS SCHLUMBERGER** [FR/FR]; 42 rue Saint Dominique, F-75007 Paris (FR).

(71) Applicant *(for GB, JP, NL only)*: **SCHLUMBERGER HOLDINGS LIMITED**; P.O. Box 71, Craigmuir Chambers, Road Town, Tortola, Virgin Islands, British, 1110 (VG).

(71) Applicant *(for all designated States except AE, AO, BH, CA, CN, FR, GB, GH, IN, JP, LY, MA, MZ, NA, NG, NL, PH, SD, SY, US, VN)*: **SCHLUMBERGER TECHNOLOGY B.V.** [NL/NL]; Parkstraat 83-89m, NL-2514 JG The Hague (NL).

(71) Applicant *(for AE, AO, BF, BH, BJ, CF, CG, CI, CM, CN, GA, GH, GN, GQ, GW, IN, KM, LY, MA, ML, MR, MZ, NA, NE, NG, PH, SD, SN, SY, TD, TG, VN only)*: **PRAD RESEARCH AND DEVELOPMENT LIMITED**; P.O. Box 71, Craigmuir Chambers, Road Town, Tortola, Virgin Island, British, 1110 (VG).

(71) Applicant *(for US only)*: **SCHLUMBERGER TECHNOLOGY CORPORATION** [US/US]; 300 Schlumberger Drive, Sugar Land, Texas 77478 (US).

(72) Inventors: **WENG, Xiaowei**; 10019 Terrance Springs Lane, Katy, Texas 77494 (US). **KRESSE, Olga**; 15270 Voss Road, # 937, Sugar Land, Texas 77478 (US).

(74) Agents: **GREENE, Rachel** et al.; 10001 Richmond Avenue, IP Administration Center of Excellence, Room 4720, Houston, Texas 77042 (US).

(81) Designated States *(unless otherwise indicated, for every kind of national protection available)*: AE, AG, AL, AM, AO, AT, AU, AZ, BA, BB, BG, BH, BN, BR, BW, BY, BZ, CA, CH, CL, CN, CO, CR, CU, CZ, DE, DK, DM, DO, DZ, EC, EE, EG, ES, FI, GB, GD, GE, GH, GM, GT, HN, HR, HU, ID, IL, IN, IR, IS, JP, KE, KG, KN, KP, KR, KZ, LA, LC, LK, LR, LS, LU, LY, MA, MD, ME, MG,

[Continued on next page]

(54) Title: MODELING OF INTERACTION OF HYDRAULIC FRACTURES IN COMPLEX FRACTURE NETWORKS

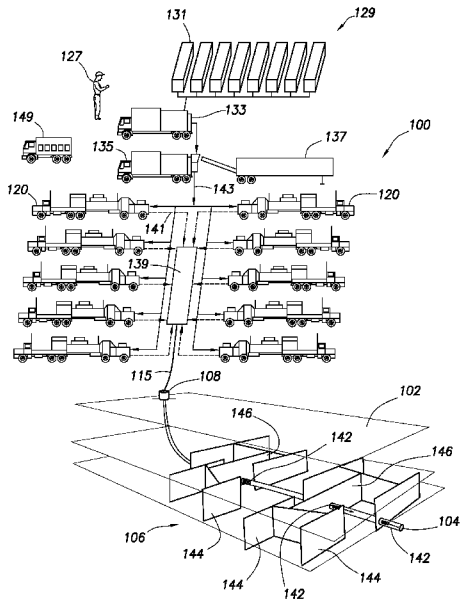

FIG. 1.1

(57) Abstract: Methods of performing a fracture operation at a wellsite with a fracture network are provided. The methods involve obtaining wellsite data and a mechanical earth model, and generating a hydraulic fracture growth pattern for the fracture network over time. The generating involves extending hydraulic fractures from a wellbore and into the fracture network of a subterranean formation to form a hydraulic fracture network, determining hydraulic fracture parameters after the extending, determining transport parameters for proppant passing through the hydraulic fracture network, and determining fracture dimensions of the hydraulic fractures from the hydraulic fracture parameters, the transport parameters and the mechanical earth model. The methods also involve performing stress shadowing on the hydraulic fractures to determine stress interference between fractures at different depths, and repeating the generating based on the determined stress interference. The methods may also involve determining crossing behavior.

WO 2015/069817 A1

MK, MN, MW, MX, MY, MZ, NA, NG, NI, NO, NZ, OM, PA, PE, PG, PH, PL, PT, QA, RO, RS, RU, RW, SA, SC, SD, SE, SG, SK, SL, SM, ST, SV, SY, TH, TJ, TM, TN, TR, TT, TZ, UA, UG, US, UZ, VC, VN, ZA, ZM, ZW.

(84) Designated States *(unless otherwise indicated, for every kind of regional protection available)*: ARIPO (BW, GH, GM, KE, LR, LS, MW, MZ, NA, RW, SD, SL, ST, SZ, TZ, UG, ZM, ZW), Eurasian (AM, AZ, BY, KG, KZ, RU, TJ, TM), European (AL, AT, BE, BG, CH, CY, CZ, DE, DK, EE, ES, FI, FR, GB, GR, HR, HU, IE, IS, IT, LT, LU, LV, MC, MK, MT, NL, NO, PL, PT, RO, RS, SE, SI, SK, SM, TR), OAPI (BF, BJ, CF, CG, CI, CM, GA, GN, GQ, GW, KM, ML, MR, NE, SN, TD, TG).

Published:

— *with international search report (Art. 21(3))*

MODELING OF INTERACTION OF HYDRAULIC FRACTURES IN COMPLEX FRACTURE NETWORKS

CROSS-REFERENCE TO RELATED APPLICATIONS

[0001] This application claims priority to US Provisional Application No. 61/900,479, filed on November 6, 2013, the entire contents of which is hereby incorporated by reference herein. This application is a continuation-in-part of US Patent Application No. 11/356,369, filed on November 2, 2012, the entire contents of which is hereby incorporated by reference herein.

BACKGROUND

[0002] The present disclosure relates generally to methods and systems for performing wellsite operations. More particularly, this disclosure is directed to methods and systems for performing fracture operations, such as investigating subterranean formations and characterizing hydraulic fracture networks in a subterranean formation.

[0003] In order to facilitate the recovery of hydrocarbons from oil and gas wells, the subterranean formations surrounding such wells can be hydraulically fractured. Hydraulic fracturing may be used to create cracks in subsurface formations to allow oil or gas to move toward the well. A formation is fractured by introducing a specially engineered fluid (referred to as "fracturing fluid" or "fracturing slurry" herein) at high pressure and high flow rates into the formation through one or more wellbores. Hydraulic fractures may extend away from the wellbore hundreds of feet in two opposing directions according to the natural stresses within the formation. Under certain circumstances, they may form a complex fracture network. Complex fracture networks can include induced hydraulic fractures and natural fractures, which may or may not intersect, along multiple azimuths, in multiple planes and directions, and in multiple regions.

[0004] Current hydraulic fracture monitoring methods and systems may map where the fractures occur and the extent of the fractures. Some methods and systems of microseismic monitoring may process seismic event locations by mapping seismic arrival times and polarization information into three-dimensional space through the use of modeled travel times and/or ray paths. These methods and systems can be used to infer hydraulic fracture propagation over time.

[0005] Patterns of hydraulic fractures created by the fracturing stimulation may be complex and may form a fracture network as indicated by a distribution of associated microseismic events. Complex hydraulic fracture networks have been developed to represent the created hydraulic fractures. Examples of fracture models are provided in US Patent/Application Nos. 6101447, 7363162, 7788074, 20080133186, 20100138196, and 20100250215.

SUMMARY

[0006] In at least one aspect, the present disclosure relates to methods of performing a fracture operation at a wellsite. The wellsite is positioned about a subterranean formation having a wellbore therethrough and a fracture network therein. The fracture network has natural fractures therein. The wellsite may be stimulated by injection of an injection fluid with proppant into the fracture network. The method involves obtaining wellsite data comprising natural fracture parameters of the natural fractures and obtaining a mechanical earth model of the subterranean formation and generating a hydraulic fracture growth pattern for the fracture network over time. The generating involves extending hydraulic fractures from the wellbore and into the fracture network of the subterranean formation to form a hydraulic fracture network including the natural fractures and the hydraulic fractures, determining hydraulic fracture parameters of the hydraulic fractures after the extending, determining transport parameters for the proppant passing through the hydraulic fracture network, and determining fracture dimensions of the hydraulic fractures from the determined hydraulic fracture parameters, the determined transport parameters and the mechanical earth model. The method also involves performing stress shadowing on the hydraulic fractures to determine stress interference between the hydraulic fractures at different depths, performing an additional stress shadowing on the hydraulic fractures to determine stress interference between the hydraulic fractures at different depths, and repeating the generating based on the determined stress interference. The method may also include analyzing stress interference between hydraulic fractures to evaluate the height growth of each fracture.

[0007] The performing stress shadowing may involve performing a first stress shadowing to determine interference between the hydraulic fractures and/or performing a second stress shadowing to determine interference between the hydraulic fractures at different depths. The

performing stress shadowing may involve performing a two dimensional displacement discontinuity method and/or performing a three dimensional displacement discontinuity method.

[0008] If the hydraulic fracture encounters a natural fracture, the method may also involve determining the crossing behavior between the hydraulic fractures and an encountered fracture based on the determined stress interference, and the repeating may involve repeating the generating based on the determined stress interference and the crossing behavior. The method may also involve stimulating the wellsite by injection of an injection fluid with proppant into the fracture network.

[0009] The method may also involve, if the hydraulic fracture encounters a natural fracture, determining the crossing behavior at the encountered natural fracture, and wherein the repeating comprises repeating the generating based on the determined stress interference and the crossing behavior. The fracture growth pattern may be altered or unaltered by the crossing behavior. A fracture pressure of the hydraulic fracture network may be greater than a stress acting on the encountered fracture, and the fracture growth pattern may propagate along the encountered fracture. The fracture growth pattern may continue to propagate along the encountered fracture until an end of the natural fracture is reached. The fracture growth pattern may change direction at the end of the natural fracture, and the fracture growth pattern may extend in a direction normal to a minimum stress at the end of the natural fracture. The fracture growth pattern may propagate normal to a local principal stress according to the stress shadowing.

[0010] The stress shadowing may involve performing displacement discontinuity for each of the hydraulic fractures. The stress shadowing may involve performing stress shadowing about multiple wellbores of a wellsite and repeating the generating using the stress shadowing performed on the multiple wellbores. The stress shadowing may involve performing stress shadowing at multiple stimulation stages in the wellbore.

[0011] The method may also involve validating the fracture growth pattern. The validating may involve comparing the fracture growth pattern with at least one simulation of stimulation of the fracture network. The method may also involve adjusting the stimulating (e.g., pumping rate and/or fluid viscosity) based on the stress shadowing.

[0012] The extending may involve extending the hydraulic fractures along a fracture growth pattern based on the natural fracture parameters and a minimum stress and a maximum stress on the subterranean formation. The determining fracture dimensions may include one of evaluating seismic measurements, ant tracking, sonic measurements, geological measurements and combinations thereof. The wellsite data may include at least one of geological, petrophysical, geomechanical, log measurements, completion, historical and combinations thereof. The natural fracture parameters may be generated by one of observing borehole imaging logs, estimating fracture dimensions from wellbore measurements, obtaining microseismic images, and combinations thereof.

BRIEF DESCRIPTION OF THE DRAWINGS

[0013] Embodiments of the system and method for characterizing wellbore stresses are described with reference to the following figures. The same numbers are used throughout the figures to reference like features and components.

[0014] Fig. 1.1 is a schematic illustration of a hydraulic fracturing site depicting a fracture operation;

[0015] Fig. 1.2 is a schematic illustration of a hydraulic fracture site with microseismic events depicted thereon;

[0016] Fig. 2 is a schematic illustration of a 2D fracture;

[0017] Figs. 3.1 and 3.2 are schematic illustrations of a stress shadow effect;

[0018] Fig. 4 is a schematic illustration comparing 2D DDM and Flac3D for two parallel straight fractures;

[0019] Figs. 5.1-5.3 are graphs illustrating 2D DDM and Flac3D of extended fractures for stresses in various positions;

[0020] Figs. 6.1-6.2 are graphs depicting propagation paths for two initially parallel fractures in isotropic and anisotropic stress fields, respectively;

[0021] Figs. 7.1-7.2 are graphs depicting propagation paths for two initially offset fractures in isotropic and anisotropic stress fields, respectively;

[0022] Fig. 8 is a schematic illustration of transverse parallel fractures along a horizontal well;

[0023] Fig. 9 is a graph depicting lengths for five parallel fractures;

[0024] Fig. 10 is a schematic diagram depicting UFM fracture geometry and width for the parallel fractures of Figure 9;

[0025] Figs. 11.1-11.2 are schematic diagrams depicting fracture geometry for a high perforation friction case and a large fracture spacing case, respectively;

[0026] Fig. 12 is a graph depicting microseismic mapping;

[0027] Figs. 13.1-13.4 are schematic diagrams illustrating a simulated fracture network compared to the microseismic measurements for stages 1-4, respectively;

[0028] Figs. 14.1-14.4 are schematic diagrams depicting a distributed fracture network at various stages;

[0029] Fig. 15 is a flow chart depicting a method of performing a fracture operation; and

[0030] Figs. 16.1-16.4 are schematic illustrations depicting fracture growth about a wellbore during a fracture operation.

[0031] Fig. 17 is a schematic diagram showing a coordinate system attached to a rectangular 3D DDM element.

[0032] Figs. 18-20 are schematic diagrams showing two vertical fractures at different depths and affecting each fracture's height growth due to stress shadowing.

[0033] Fig. 21 is a flow chart depicting another method of performing a fracture operation.

DETAILED DESCRIPTION

[0034] The description that follows includes exemplary apparatuses, methods, techniques, and

instruction sequences that embody techniques of the inventive subject matter. However, it is understood that the described embodiments may be practiced without these specific details.

[0035] Models have been developed to understand subsurface fracture networks. The models may consider various factors and/or data, but may not be constrained by accounting for either the amount of pumped fluid or mechanical interactions between fractures and injected fluid and among the fractures. Constrained models may be provided to give a fundamental understanding of involved mechanisms, but may be complex in mathematical description and/or require computer processing resources and time in order to provide accurate simulations of hydraulic fracture propagation. A constrained model may be configured to perform simulations to consider factors, such as interaction between fractures, over time and under desired conditions.

[0036] An unconventional fracture model (UFM) (or complex model) may be used to simulate complex fracture network propagation in a formation with pre-existing natural fractures. Multiple fracture branches can propagate simultaneously and intersect/cross each other. Each open fracture may exert additional stresses on the surrounding rock and adjacent fractures, which may be referred to as "stress shadow" effect. The stress shadow can cause a restriction of fracture parameters (e.g., width), which may lead to, for example, a greater risk of proppant screenout. The stress shadow can also alter the fracture propagation path and affect fracture network patterns. The stress shadow may affect the modeling of the fracture interaction in a complex fracture model.

[0037] A method for computing the stress shadow in a complex hydraulic fracture network is presented. The method may be performed based on an enhanced 2D Displacement Discontinuity Method (2D DDM) with correction for finite fracture height or 3D Displacement Discontinuity Method (3D DDM). The computed stress field from 2D DDM may be compared to 3D numerical simulation (3D DDM or flac3D) to determine an approximation for the 3D fracture problem. This stress shadow calculation may be incorporated in the UFM. The results for simple cases of two fractures shows the fractures can either attract or expel each other depending, for example, on their initial relative positions, and may be compared with an independent 2D non-planar hydraulic fracture model. Stress shadowing may also be provided, using for example 3D DDM, to take into consideration interaction of fractures at different depths.

[0038] Additional examples of both planar and complex fractures propagating from multiple perforation clusters are presented, showing that fracture interaction may control the fracture dimension and propagation pattern. In a formation with small stress anisotropy, fracture interaction can lead to dramatic divergence of the fractures as they may tend to repel each other. However, even when stress anisotropy is large and fracture turning due to fracture interaction is limited, stress shadowing may have an effect on fracture width, which may affect the injection rate distribution into multiple perforation clusters, and hence overall fracture network geometry and proppant placement.

[0039] Figures 1.1 and 1.2 depict fracture propagation about a wellsite 100. The wellsite has a wellbore 104 extending from a wellhead 108 at a surface location and through a subterranean formation 102 therebelow. A fracture network 106 extends about the wellbore 104. A pump system 129 is positioned about the wellhead 108 for passing fluid through tubing 142.

[0040] The pump system 129 is depicted as being operated by a field operator 127 for recording maintenance and operational data and/or performing the operation in accordance with a prescribed pumping schedule. The pumping system 129 pumps fluid from the surface to the wellbore 104 during the fracture operation.

[0041] The pump system 129 may include a water source, such as a plurality of water tanks 131, which feed water to a gel hydration unit 133. The gel hydration unit 133 combines water from the tanks 131 with a gelling agent to form a gel. The gel is then sent to a blender 135 where it is mixed with a proppant from a proppant transport 137 to form a fracturing fluid. The gelling agent may be used to increase the viscosity of the fracturing fluid, and to allow the proppant to be suspended in the fracturing fluid. It may also act as a friction reducing agent to allow higher pump rates with less frictional pressure.

[0042] The fracturing fluid is then pumped from the blender 135 to the treatment trucks 120 with plunger pumps as shown by solid lines 143. Each treatment truck 120 receives the fracturing fluid at a low pressure and discharges it to a common manifold 139 (sometimes called a missile trailer or missile) at a high pressure as shown by dashed lines 141. The missile 139 then directs the fracturing fluid from the treatment trucks 120 to the wellbore 104 as shown by solid line 115. One or more treatment trucks 120 may be used to supply fracturing fluid at a desired rate.

[0043] Each treatment truck 120 may be normally operated at any rate, such as well under its maximum operating capacity. Operating the treatment trucks 120 under their operating capacity may allow for one to fail and the remaining to be run at a higher speed in order to make up for the absence of the failed pump. A computerized control system 149 may be employed to direct the entire pump system 129 during the fracturing operation.

[0044] Various fluids, such as conventional stimulation fluids with proppants, may be used to create fractures. Other fluids, such as viscous gels, "slick water" (which may have a friction reducer (polymer) and water) may also be used to hydraulically fracture shale gas wells. Such "slick water" may be in the form of a thin fluid (e.g., nearly the same viscosity as water) and may be used to create more complex fractures, such as multiple micro-seismic fractures detectable by monitoring.

[0045] As also shown in Figures 1.1 and 1.2, the fracture network includes fractures located at various positions around the wellbore 104. The various fractures may be natural fractures 144 present before injection of the fluids, or hydraulic fractures 146 generated about the formation 102 during injection. Figure 1.2 shows a depiction of the fracture network 106 based on microseismic events 148 gathered using conventional means.

[0046] Multi-stage stimulation may be the norm for unconventional reservoir development. However, an obstacle to optimizing completions in shale reservoirs may involve a lack of hydraulic fracture models that can properly simulate complex fracture propagation often observed in these formations. A complex fracture network model (or UFM), has been developed (*see, e.g., Weng, X., Kresse, O., Wu, R., and Gu, H., Modeling of Hydraulic Fracture Propagation in a Naturally Fractured Formation. Paper SPE 140253 presented at the SPE Hydraulic Fracturing Conference and Exhibition, Woodlands, Texas, USA, January 24–26 (2011)* (hereafter "Weng 2011"); *Kresse, O., Cohen, C., Weng, X., Wu, R., and Gu, H. 2011* (hereafter "Kresse 2011"). *Numerical Modeling of Hydraulic Fracturing in Naturally Fractured Formations. 45th US Rock Mechanics/Geomechanics Symposium, San Francisco, CA, June 26-29*, the entire contents of which are hereby incorporated herein).

[0047] Existing models may be used to simulate fracture propagation, rock deformation, and fluid flow in the complex fracture network created during a treatment. The model may also be

used to solve the fully coupled problem of fluid flow in the fracture network and the elastic deformation of the fractures, which may have similar assumptions and governing equations as conventional pseudo-3D fracture models. Transport equations may be solved for each component of the fluids and proppants pumped.

[0048] Conventional planar fracture models may model various aspects of the fracture network. The provided UFM may also involve the ability to simulate the interaction of hydraulic fractures with pre-existing natural fractures, i.e. determine whether a hydraulic fracture propagates through or is arrested by a natural fracture when they intersect and subsequently propagates along the natural fracture. The branching of the hydraulic fracture at the intersection with the natural fracture may give rise to the development of a complex fracture network.

[0049] A crossing model may be extended from Renshaw and Pollard (*see, e.g., Renshaw, C. E. and Pollard, D. D. 1995, An Experimentally Verified Criterion for Propagation across Unbounded Frictional Interfaces in Brittle, Linear Elastic Materials. Int. J. Rock Mech. Min. Sci. & Geomech. Abstr., 32: 237-249 (1995)* the entire contents of which is hereby incorporated herein) interface crossing criterion, to apply to any intersection angle, and may be developed (*see, e.g., Gu, H. and Weng, X. Criterion for Fractures Crossing Frictional Interfaces at Non-orthogonal Angles. 44th US Rock symposium, Salt Lake City, Utah, June 27-30, 2010* (hereafter "Gu and Weng 2010"), the entire contents of which are hereby incorporated by reference herein) and validated against experimental data (*see, e.g., Gu, H., Weng, X., Lund, J., Mack, M., Ganguly, U. and Suarez-Rivera R. 2011. Hydraulic Fracture Crossing Natural Fracture at Non-Orthogonal Angles, A Criterion, Its Validation and Applications. Paper SPE 139984 presented at the SPE Hydraulic Fracturing Conference and Exhibition, Woodlands, Texas, January 24-26* (2011) (hereafter "Gu et al. 2011"), the entire contents of which are hereby incorporated by reference herein), and integrated in the UFM.

[0050] To properly simulate the propagation of multiple or complex fractures, the fracture model may take into account an interaction among adjacent hydraulic fracture branches, often referred to as the "stress shadow" effect. When a single planar hydraulic fracture is opened under a finite fluid net pressure, it may exert a stress field on the surrounding rock that is proportional to the net pressure.

[0051] In the limiting case of an infinitely long vertical fracture of a constant finite height, an analytical expression of the stress field exerted by the open fracture may be provided. See, .e.g., *Warpinski, N.F. and Teufel, L.W., Influence of Geologic Discontinuities on Hydraulic Fracture Propagation, JPT, Feb., 209-220 (1987)* (hereafter "Warpinski and Teufel") and *Warpinski, N.R., and Branagan, P.T., Altered-Stress Fracturing. SPE JPT, September, 1989, 990-997 (1989)*, the entire contents of which are hereby incorporated by reference herein. The net pressure (or more precisely, the pressure that produces the given fracture opening) may exert a compressive stress in the direction normal to the fracture on top of the minimum in-situ stress, which may equal the net pressure at the fracture face, but quickly falls off with the distance from the fracture.

[0052] At a distance beyond one fracture height, the induced stress may be a small fraction of the net pressure. Thus, the term "stress shadow" may be used to describe this increase of stress in the region surrounding the fracture. If a second hydraulic fracture is created parallel to an existing open fracture, and if it falls within the "stress shadow" (i.e. the distance to the existing fracture is less than the fracture height), the second fracture may, in effect, see a closure stress greater than the original in-situ stress. As a result, a higher pressure may be needed to propagate the fracture, and/or the fracture may have a narrower width, as compared to the corresponding single fracture.

[0053] One application of the stress shadow study may involve the design and optimization of the fracture spacing between multiple fractures propagating simultaneously from a horizontal wellbore. In ultra low permeability shale formations, fractures may be closely spaced for effective reservoir drainage. However, the stress shadow effect may prevent a fracture propagating in close vicinity of other fractures (*see, e.g., Fisher, M.K., J.R. Heinze, C.D. Harris, B.M. Davidson, C.A. Wright, and K.P. Dunn, Optimizing horizontal completion techniques in the Barnett Shale using microseismic fracture mapping. SPE 90051 presented at the SPE Annual Technical Conference and Exhibition, Houston, 26-29 September 2004,* the entire contents of which are hereby incorporated by reference herein in its entirety).

[0054] The interference between parallel fractures has been studied in the past (*see, e.g., Warpinski and Teufel; Britt, L.K. and Smith, M.B., Horizontal Well Completion, Stimulation*

Optimization, and Risk Mitigation. Paper SPE 125526 presented at the 2009 SPE Eastern Regional Meeting, Charleston, September 23-25, 2009; Cheng, Y. 2009. Boundary Element Analysis of the Stress Distribution around Multiple Fractures: Implications for the Spacing of Perforation Clusters of Hydraulically Fractured Horizontal Wells. Paper SPE 125769 presented at the 2009 SPE Eastern Regional Meeting, Charleston, September 23-25, 2009; Meyer, B.R. and Bazan, L.W., A Discrete Fracture Network Model for Hydraulically Induced Fractures: Theory, Parametric and Case Studies. Paper SPE 140514 presented at the SPE Hydraulic Fracturing Conference and Exhibition, Woodlands, Texas, USA, January 24–26, 2011; Roussel, N.P. and Sharma, M.M, Optimizing Fracture Spacing and Sequencing in Horizontal-Well Fracturing, SPEPE, May, 2011, pp. 173-184, the entire contents of which are hereby incorporated by reference herein*)*. The studies may involve parallel fractures under static conditions.

[0055] An effect of stress shadow may be that the fractures in the middle region of multiple parallel fractures may have smaller width because of the increased compressive stresses from neighboring fractures *(see, e.g., Germanovich, L.N., and Astakhov D., Fracture Closure in Extension and Mechanical Interaction of Parallel Joints. J. Geophys. Res., 109, B02208, doi: 10.1029/2002 JB002131 (2004); Olson, J.E., Multi-Fracture Propagation Modeling: Applications to Hydraulic Fracturing in Shales and Tight Sands. 42nd US Rock Mechanics Symposium and 2nd US-Canada Rock Mechanics Symposium, San Francisco, CA, June 29 – July 2, 2008*, the entire contents of which are hereby incorporated by reference herein). When multiple fractures are propagating simultaneously, the flow rate distribution into the fractures may be a dynamic process and may be affected by the net pressure of the fractures. The net pressure may be strongly dependent on fracture width, and hence, the stress shadow effect on flow rate distribution and fracture dimensions warrants further study.

[0056] The dynamics of simultaneously propagating multiple fractures may also depend on the relative positions of the initial fractures. If the fractures are parallel, e.g. in the case of multiple fractures that are orthogonal to a horizontal wellbore, the fractures may repel each other, resulting in the fractures curving outward. However, if the multiple fractures are arranged in an en echlon pattern, e.g. for fractures initiated from a horizontal wellbore that is not orthogonal to the fracture plane, the interaction between the adjacent fractures may be such that their tips

attract each other and even connect (*see, e.g., Olson, J. E. Fracture Mechanics Analysis of Joints and Veins. PhD dissertation, Stanford University, San Francisco, California (1990); Yew, C.H., Mear, M.E., Chang, C.C., and Zhang, X.C. On Perforating and Fracturing of Deviated Cased Wellbores. Paper SPE 26514 presented at SPE 68th Annual Technical Conference and Exhibition, Houston, TX, Oct. 3-6 (1993); Weng, X., Fracture Initiation and Propagation from Deviated Wellbores. Paper SPE 26597 presented at SPE 68th Annual Technical Conference and Exhibition, Houston, TX, Oct. 3-6 (1993)*, the entire contents of which are hereby incorporated by reference herein).

[0057] When a hydraulic fracture intersects a secondary fracture oriented in a different direction, it may exert an additional closure stress on the secondary fracture that is proportional to the net pressure. This stress may be derived and be taken into account in the fissure opening pressure calculation in the analysis of pressure-dependent leakoff in fissured formation (*see, e.g., Nolte, K., Fracturing Pressure Analysis for nonideal behavior. JPT, Feb. 1991, 210-218 (SPE 20704)* (1991) (hereafter "Nolte 1991"), the entire contents of which are hereby incorporated by reference herein).

[0058] For more complex fractures, a combination of various fracture interactions as discussed above may be present. To properly account for these interactions and remain computationally efficient so it can be incorporated in the complex fracture network model, a proper modeling framework may be constructed. A method based on an enhanced 2D Displacement Discontinuity Method (2D DDM) may be used for computing the induced stresses on a given fracture and in the rock from the rest of the complex fracture network (*see, e.g., Olson, J.E., Predicting Fracture Swarms – The Influence of Sub critical Crack Growth and the Crack-Tip Process Zone on Joints Spacing in Rock. In The Initiation, Propagation and Arrest of Joints and Other Fractures, ed. J.W.Cosgrove and T.Engelder, Geological Soc. Special Publications, London, 231, 73-87 (2004)*(hereafter "Olson 2004"), the entire contents of which are hereby incorporated by reference herein). Fracture turning may also be modeled based on the altered local stress direction ahead of the propagating fracture tip due to the stress shadow effect. The simulation results from the UFM model that incorporates the fracture interaction modeling are presented.

UFM Model Description

[0059] To simulate the propagation of a complex fracture network that consists of many intersecting fractures, equations governing the underlying physics of the fracturing process may be used. The basic governing equations may include, for example, equations governing fluid flow in the fracture network, the equation governing the fracture deformation, and the fracture propagation/interaction criterion.

[0060] Continuity equation assumes that fluid flow propagates along a fracture network with the following mass conservation:

$$\frac{\partial q}{\partial s} + \frac{\partial (H_{fl}\overline{w})}{\partial t} + q_L = 0 \qquad (1)$$

where q is the local flow rate inside the hydraulic fracture along the length, $\overline{w}$ is an average width or opening at the cross-section of the fracture at position $s=s(x,y)$, H_{fl} is the height of the fluid in the fracture, and q_L is the leak-off volume rate through the wall of the hydraulic fracture into the matrix per unit height (velocity at which fracturing fluid infiltrates into surrounding permeable medium) which is expressed through Carter's leak-off model. The fracture tips propagate as a sharp front, and the length of the hydraulic fracture at any given time t is defined as $l(t)$.

[0061] The properties of driving fluid may be defined by power-law exponent n′ (fluid behavior index) and consistency index K′. The fluid flow could be laminar, turbulent or Darcy flow through a proppant pack, and may be described correspondingly by different laws. For the general case of 1D laminar flow of power-law fluid in any given fracture branch, the Poiseuille law (see, e.g., Nolte, 1991) may be used:

$$\frac{\partial p}{\partial s} = -\alpha_0 \frac{1}{\overline{w}^{2n'+1}} \frac{q}{H_{fl}} \left| \frac{q}{H_{fl}} \right|^{n'-1} \qquad (2)$$

where

$$\alpha_0 = \frac{2K'}{\phi(n')^{n'}} \cdot \left(\frac{4n'+2}{n'}\right)^{n'}; \quad \phi(n') = \frac{1}{H_{fl}} \int_{H_{fl}} \left(\frac{w(z)}{\overline{w}}\right)^{\frac{2n'+1}{n'}} dz \tag{3}$$

Here *w(z)* represents fracture width as a function of depth at current position *s*, α is coefficient, n' is power law exponent (fluid consistency index), ϕ is shape function, and dz is the integration increment along the height of the fracture in the formula.

[0062] Fracture width may be related to fluid pressure through the elasticity equation. The elastic properties of the rock (which may be considered as homogeneous, isotropic, linear elastic material) may be defined by Young's modulus *E* and Poisson's ratio ν. For a vertical fracture in a layered medium with variable minimum horizontal stress $\sigma_h(x, y, z)$ and fluid pressure *p*, the width profile (*w*) can be determined from an analytical solution given as:

$$w(x, y, z) = w(p(x, y), H, z) \tag{4}$$

where W is the fracture width at a point with spatial coordinates x, y, z (coordinates of the center of fracture element); p(x,y) is the fluid pressure, H is the fracture element height, and z is the vertical coordinate along fracture element at point (x,y).

[0063] Because the height of the fractures may vary, the set of governing equations may also include the height growth calculation as described, for example, in Kresse 2011.

[0064] In addition to equations described above, the global volume balance condition may be satisfied:

$$\int_0^t Q(t)dt = \int_0^{L(t)} H(s,t)\overline{w}(s,t)ds + \int_{H_L} \int_0^t \int_0^{L(t)} 2g_L ds dt dh_l \tag{5}$$

where g_L is fluid leakoff velocity, Q(t) is time dependent injection rate, H(s,t) height of the fracture at spacial point s(x,y) and at the time t, ds is length increment for integration along fracture length, d_t is time increment, dh_l is increment of leakoff height, H_L is leakoff height, an s_0 is a spurt loss coefficient. Equation (5) provides that the total volume of fluid pumped during time *t* is equal to the volume of fluid in the fracture network and the volume leaked from the

fracture up to time t. Here $L(t)$ represents the total length of the HFN at the time t and S_0 is the spurt loss coefficient. The boundary conditions may require the flow rate, net pressure and fracture width to be zero at all fracture tips.

[0065] The system of Eq. 1 – 5, together with initial and boundary conditions, may be used to represent a set of governing equations. Combining these equations and discretizing the fracture network into small elements may lead to a nonlinear system of equations in terms of fluid pressure p in each element, simplified as $f(p) = 0$, which may be solved by using a damped Newton-Raphson method.

[0066] Fracture interaction may be taken into account to model hydraulic fracture propagation in naturally fractured reservoirs. This includes, for example, the interaction between hydraulic fractures and natural fractures, as well as interaction between hydraulic fractures. For the interaction between hydraulic and natural fractures a semi-analytical crossing criterion may be implemented in the UFM using, for example, the approach described in Gu and Weng 2010, and Gu et al. 2011.

Modeling of Stress Shadow

[0067] For parallel fractures, the stress shadow can be represented by the superposition of stresses from neighboring fractures. Figure 2 is a schematic depiction of a 2D fracture 200 about a coordinate system having an x-axis and a y-axis. Various points along the 2D fractures, such as a first end at h/2, a second end at –h/2 and a midpoint are extended to an observation point (x,y). Each line L extends at angles θ_1, θ_2 from the points along the 2D fracture to the observation point.

[0068] The stress field around a 2D fracture with internal pressure p can be calculated using, for example, the techniques as described in Warpinski and Teufel. The stress that affects fracture width is σ_x, and can be calculated from:

$$\sigma_x = p\left[1 - \frac{\bar{L}}{\sqrt{\bar{L}_1\bar{L}_2}}cos\left(\theta - \frac{\theta_1+\theta_2}{2}\right) - \frac{\bar{L}}{(\bar{L}_1\bar{L}_2)^{\frac{3}{2}}}sin\theta sin\left(\frac{3}{2}(\theta_1+\theta_2)\right)\right] \quad (6)$$

where

$$\theta = arctan\left(-\frac{\bar{x}}{\bar{y}}\right)$$

$$\theta_1 = arctan\left(-\frac{\bar{x}}{\overline{\overline{1+\bar{y}}}}\right)$$

$$\theta_2 = arctan\left(\frac{\bar{x}}{1-\bar{y}}\right) \quad (7)$$

and where σ_x is stress in the x direction, p is internal pressure, and $\bar{x}, \bar{y}, \bar{L}, \bar{L}_1, \bar{L}_2$ are the coordinates and distances in Figure 2 normalized by the fracture half-height *h/2*. Since σ_x varies in the y-direction as well as in the x-direction, an averaged stress over the fracture height may be used in the stress shadow calculation.

[0069] The analytical equation given above can be used to compute the average effective stress of one fracture on an adjacent parallel fracture and can be included in the effective closure stress on that fracture.

[0070] For more complex fracture networks, the fractures may orient in different directions and intersect each other. Figure 3.1 shows a complex fracture network 300 depicting stress shadow effects. The fracture network 300 includes hydraulic fractures 303 extending from a wellbore 304 and interacting with other fractures 305 in the fracture network 300.

[0071] A more general approach may be used to compute the effective stress on any given fracture branch from the rest of the fracture network. In UFM, the mechanical interactions between fractures may be modeled based on an enhanced 2D Displacement Discontinuity Method (DDM) (Olson 2004) for computing the induced stresses (see, e.g., Figure 3.2).

[0072] In a 2D, plane-strain, displacement discontinuity solution, (*see, e.g., Crouch, S.L. and Starfield, A.M., Boundary Element Methods in Solid Mechanics, George Allen & Unwin Ltd, London. Fisher, M.K. (1983)*(hereafter Crouch and Starfield 1983), the entire contents of which are hereby incorporated by reference) may be used to describe the normal and shear stresses (σ_n and σ_s) acting on one fracture element induced by the opening and shearing displacement discontinuities (D_n and D_s) from all fracture elements. To account for the 3D effect due to finite fracture height, Olson 2004 may be used to provide a 3D correction factor to the influence

coefficients C^{ij} in combination with the modified elasticity equations of 2D DDM as follows:

$$\sigma_n^i = \sum_{j=1}^{N} A^{ij} C_{ns}^{ij} D_s^j + \sum_{j=1}^{N} A^{ij} C_{nn}^{ij} D_n^j$$
$$\sigma_s^i = \sum_{j=1}^{N} A^{ij} C_{ss}^{ij} D_s^j + \sum_{j=1}^{N} A^{ij} C_{sn}^{ij} D_n^j \qquad (8)$$

where A is a matrix of influence coefficients described in eq. (9), N is a total number of elements in the network whose interaction is considered, i is the element considered, and j=1, N are other elements in the network whose influence on the stresses on element *i* are calculated; and where C^{ij} are the 2D, plane-strain elastic influence coefficients. These expressions can be found in Crouch and Starfield 1983.

[0073] Elem i and j of Figure 3.2 schematically depict the variables i and j in equation (8). Discontinuities D_s and D_n applied to Elem j are also depicted in Figure 3.2. Dn may be the same as the fracture width, and the shear stress *s* may be 0 as depicted. Displacement discontinuity from Elem j creates a stress on Elem i as depicted by σ_s and σ_n.

[0074] The 3D correction factor suggested by Olson 2004 may be presented as follows:

$$A^{ij} = 1 - \frac{d_{ij}^{\beta}}{\left[d_{ij}^2 + (h/\alpha)^2\right]^{\beta/2}} \qquad (9)$$

where h is the fracture height, d_{ij} is the distance between elements i and j, α and β are fitting parameters. Eq. 9 shows that the 3D correction factor may lead to decaying of interaction between any two fracture elements when the distance increases.

[0075] In the UFM model, at each time step, the additional induced stresses due to the stress shadow effects may be computed. It may be assumed that at any time, fracture width equals the normal displacement discontinuities (D_n) and shear stress at the fracture surface is zero, i.e., $D_n^j = w_j$, $\sigma_s^i = 0$. Substituting these two conditions into Eq. 8, the shear displacement discontinuities (D_s) and normal stress induced on each fracture element (σ_n) may be found.

[0076] The effects of the stress shadow induced stresses on the fracture network propagation pattern may be described in two folds. First, during pressure and width iteration, the original in-situ stresses at each fracture element may be modified by adding the additional normal stress due to the stress shadow effect. This may directly affect the fracture pressure and width distribution which may result in a change on the fracture growth. Second, by including the stress shadow induced stresses (normal and shear stresses), the local stress fields ahead of the propagating tips may also be altered which may cause the local principal stress direction to deviate from the original in-situ stress direction. This altered local principal stress direction may result in the fracture turning from its original propagation plane and may further affect the fracture network propagation pattern.

3D Displacement Discontinuity Method (3D DDM)

[0077] In addition to the enhanced 2D DDM method described herein, a method based on 3D DDM can be used for various applications. For a given hydraulic fracture network that is discretized into connected small rectangular elements, any given rectangular element may be subjected to displacement discontinuity between two faces of the rectangular element represented by *Dx*, *Dy*, and *Dz*, and the induced stresses in the rock at any point (*x*, *y*, *z*) can be computed using the 3D DDM solution presented herein.

[0078] Figure 17 shows a schematic diagram 1700 of a local x,y,z coordinate system for a rectangular element 1740 in an x-y plane. This figure depicts a fracture plane about the coordinate axis. The induced displacement and stress field can be expressed as:

$$u_x = [2(1-\nu)f_{,z} - zf_{,xx}]D_x - zf_{,xy}D_y - [(1-2\nu)f_{,x} + zf_{,xz}]D_z \quad (10)$$

$$u_y = -zf_{,xy}D_x + [2(1-\nu)f_{,z} - zf_{,yy}]D_y - [(1-2\nu)f_{,y} + zf_{,yz}]D_z \quad (11)$$

$$u_z = [(1-2\nu)f_{,x} - zf_{,xz}]D_x + [(1-2\nu)f_{,y} - zf_{,yz}]D_y + [2(1-\nu)f_{,z} - zf_{,zz}]D_z \quad (12)$$

$$\sigma_{xx} = 2G\{[2f_{,xz} - zf_{,xxz}]D_x + [2\nu f_{,yz} - zf_{,xxy}]D_y + [f_{,zz} + (1-2\nu)f_{,yy} - zf_{,xxz}]D_z\} \quad (13)$$

$$\sigma_{yy} = 2G\{[2\nu f_{,xz} - zf_{,xyy}]D_x + [2f_{,yz} - zf_{,yyy}]D_y + [f_{,zz} + (1-2\nu)f_{,xx} - zf_{,yyz}]D_z\} \quad (14)$$

$$\sigma_{zz} = 2G\{-zf_{,xxz}D_x - zf_{,yyz}]D_y + [f_{,zz} - zf_{,zzz}]D_z\} \quad (15)$$

$$\tau_{xy} = 2G\{[(1-\nu)f_{,yz} - zf_{,xxy}]D_x + [(1-\nu)f_{,xz} - zf_{,xyy}]D_y - [(1-2\nu)f_{,xy} + zf_{,xyz}]D_z\} \quad (16)$$

$$\tau_{yz} = 2G\{-[\nu f_{,xy} + zf_{,xyz}]D_x + [f_{,zz} + \nu f_{,yy} - zf_{,yyz}]D_y - zf_{,yzz}D_z\} \quad (17)$$

$$\tau_{xz} = 2G\{[(f_{,zz} + \nu f_{,yy} - zf_{,xxz}]D_x - [\nu f_{,xy} + zf_{,xyz}]D_y - zf_{,xzz}D_z\} \quad (18)$$

Where a and b are the half lengths of the edges of the rectangle, the induced displacement and stress field can be expressed as follows:

$$f(x,y,z) = \frac{1}{8\pi(1-\nu)} \iint_A [(x-\xi)^2 + (y-\eta)^2 + z^2]^{-1/2} d\xi d\eta, \quad |\xi| \le a, |\eta| \le b \quad (19)$$

where A is the area of the rectangle, (x,y,z) is the coordinate system originated at the element, (ξ,η,0) are coordinates at point P, and ν is Poisson's ratio.

[0079] For any given observation point P(*x*,*y*,*z*) in the 3D space, the induced stress at the point P (x,y,z) with production rate Q(ξ,η,0) may be computed by superposing the stresses from all fracture elements, and by applying a coordinate transform. Example techniques involving 3D DDM are provided in Crouch, S.L. and Starfield, A.M. (1990), *Boundary Element Methods in Solid Mechanics*, Unwin Hyman, London, the entire contents of which are hereby incorporated by reference herein.

[0080] Interaction among multiple propagating hydraulic fractures, or the herein referenced stress shadow effect, can influence the fracture height growth for fractures propagating in the same layer or different layers in depth, which may have implications on the success of a fracture treatment.

[0081] In at least one embodiment of the hydraulic fracture model described herein, the model may additionally integrate the 3D DDM for computing the induced 3D stress field surrounding the propagating hydraulic fractures, and may incorporate the induced stress change along the vertical depth into a fracture height calculation of the fracture model.

[0082] For example, for two parallel fractures 1811.1, 1811.2, as illustrated in the schematic diagram 1800 of Fig. 18, the height growth may be promoted or suppressed depending on the relative fracture height. For fractures initiated from different depths, the presence of the adjacent fracture can help prevent one fracture from growing into the layer occupied by the other fracture due to the vertical stress shadowing effect. For example, due to interaction between the fractures 1811.1, 1811.2 at different depths, fracture 1811.1 may grow in an upward direction and fracture 1811.2 may grow in a downward direction as indicated by the arrows.

Validation of Stress Shadow Model

[0083] Validation of the UFM model for the cases of bi-wing fractures may be performed using, for example, Weng 2011 or Kresse 2011. Validation may also be performed using the stress shadow modeling approach. By way of example, the results may be compared using 2D DDM to Flac 3D as provided in *Itasca Consulting Group Inc., 2002, FLAC3D (Fast Lagrangian Analysis of Continua in 3 Dimensions), Version 2.1, Minneapolis: ICG (2002)* (hereafter "Itasca, 2002").

Comparison of Enhanced 2D DDM to Flac3D

[0084] The 3D correction factors suggested by Olson 2004 contain two empirical constants, α and β. The values of α and β may be calibrated by comparing stresses obtained from numerical solutions (enhanced 2D DDM) to the analytical solution for a plane-strain fracture with infinite length and finite height. The model may further be validated by comparing the 2D DDM results to a full three dimensional numerical solutions, utilizing, for example, FLAC3D, for two parallel straight fractures with finite lengths and heights.

[0085] The validation problem is shown in Figure 4. Figure 4 depicts a schematic diagram 400 comparing enhanced 2D DDM to Flac3D for two parallel straight fractures. As shown in Figure 400, two parallel fractures 407.1, 407.2 are subject to stresses σ_x, σ_y along an x, y coordinate axis. The fractures have length $2L_{xf}$, and pressure of the fracture p_1, p_2, respectively. The fractures are a distance *s* apart.

[0086] The fracture in Flac3D may be simulated as two surfaces at the same location but with un-attached grid points. Constant internal fluid pressure may be applied as the normal stress on the grids. Fractures may also be subject to remote stresses, σ_x and σ_y. Two fractures may have

the same length and height with the ratio of height/half-length = 0.3.

[0087] Stresses along x-axis (y = 0) and y-axis (x = 0) may be compared. Two closely spaced fractures (s/h = 0.5) may be simulated as shown in the comparison of Figures 5.1-5.3. These figures provide a comparison of extended 2D DDM to Flac3D: Stresses along x-axis (y = 0) and y-axis (x = 0).

[0088] These figures include graphs 500.1, 500.2, 500.3, respectively, illustrating 2D DDM and Flac3D of extended fractures for σy along the y-axis, σx along the y-axis, and σy along the x-axis, respectively. Figure 5.1 plots σy/p (y-axis) versus normalized distance from fracture (x-axis) using 2D DDM and Flac3D. Figure 5.2 plots σx/p (y-axis) versus normalized distance from fracture (x-axis) using 2D DDM and Flac3D. Figure 5.3 plots σy/p (y-axis) versus normalized distance from fracture (x-axis) using 2D DDM and Flac3D. The location L_f of the fracture tip is depicted along line x/h.

[0089] As shown in Figures 5.1-5.3, the stresses simulated from enhanced 2D DDM approach with 3D correction factor match pretty well to those from the full 3D simulator results, which indicates that the correction factor allows capture the 3D effect from the fracture height on the stress field.

Comparison to CSIRO model

[0090] The UFM model that incorporates the enchanced 2DDM approach may be validated against full 2D DDM simulator by CSIRO (*see, e.g., Zhang, X., Jeffrey, R.G., and Thiercelin, M. 2007. Deflection and Propagation of Fluid-Driven Fractures at Frictional Bedding Interfaces: A Numerical Investigation. Journal of Structural Geology, 29: 396-410,* (hereafter "Zhang 2007") the entire contents of which is hereby incorporated by reference in its entirety). This approach may be used, for example, in the limiting case of very large fracture height where 2D DDM approaches do not consider 3D effects of the fractures height.

[0091] The comparison of influence of two closely propagating fractures on each other's propagation paths may be employed. The propagation of two hydraulic fractures initiated parallel to each other (propagating along local max stress direction) may be simulated for configurations, such as: 1) initiation points on top of each other and offset from each other for isotropic, and 2)

anisotropic far field stresses. The fracture propagation path and pressure inside of each fracture may be compared for UFM and CSIRO code for the input data given in Table 1.

Injection rate	0.106m3/s	40 bbl/min
Stress anisotropy	0.9MPa	130 psi
Young's modulus	3 x 10^10Pa	4.35e+6 psi
Poisson's ratio	0.35	0.35
Fluid viscosity	0.001pa-s	1 cp
Fluid Specific Gravity	1.0	1.0
Min horizontal stress	46.7MPa	6773 psi
Max horizontal stress	47.6MPa	6903 psi
Fracture toughness	1MPa-$m^{0.5}$	1000 psi/$in^{0.5}$
Fracture height	120m	394 ft

Table 1 Input data for validation against CSIRO model

[0092] When two fractures are initiated parallel to each other with initiation points separated by $dx = 0$, $dy = 33$ ft (10.1 m) (max horizontal stress field is oriented in x-direction), they may turn away from each other due to the stress shadow effect.

[0093] The propagation paths for isotropic and anisotropic stress fields are shown in Figures 6.1 and 6.2. These figures are graphs 600.1, 600.2 depicting propagation paths for two initially parallel fractures 609.1, 609.2 in isotropic and anisotropic stress fields, respectively. The fractures 609.1 and 609.2 are initially parallel near the injection points 615.1, 615.2, but diverge as they extend away therefrom. Comparing with isotropic case, the curvatures of the fractures in the case of stress anisotropy are depicted as being smaller. This may be due to the competition between the stress shadow effect which tends to turn fractures away from each other, and far–field stresses which pushes fractures to propagate in the direction of maximum horizontal stress (x-direction). The influence of far-field stress becomes dominant as the distance between the fractures increases, in which case the fractures may tend to propagate parallel to maximum horizontal stress direction.

[0094] Figures 7.1 and 7.2 depict graphs 700.1, 7002 showing a pair of fractures initiated from two different injection points 711.1, 711.2, respectively. These figures show a comparison for the case when fractures are initiated from points separated by a distance $dx = dy = (10.1\text{m})$ for an isotropic and anisotropic stress field, respectively. In these figures, the fractures 709.1, 709.2

tend to propagate towards each other. Examples of similar type of behavior have been observed in lab experiments (*see, e.g.*, Zhang 2007).

[0095] As indicated above, the enchanced 2D DDM approach implemented in UFM model may be able to capture the 3D effects of finite fracture height on fracture interaction and propagation pattern, while being computationally efficient. A good estimation of the stress field for a network of vertical hydraulic fractures and fracture propagation direction (pattern) may be provided.

Example cases

Case #1 Parallel fractures in horizontal wells

[0096] Figure 8 is a schematic plot 800 of parallel transverse fractures 811.1, 811.2, 811.3 propagating simultaneously from multiple perforation clusters 815.1, 815.2, 815.3, respectively, about a horizontal wellbore 804. Each of the fractures 811.1, 811.2, 811.3 provides a different flow rate q_1, q_2, q_3 that is part of the total flow q_t at a pressure p_0.

[0097] When the formation condition and the perforations are the same for all the fractures, the fractures may have about the same dimensions if the friction pressure in the wellbore between the perforation clusters is proportionally small. This may be assumed where the fractures are separated far enough and the stress shadow effects are negligible. When the spacing between the fractures is within the region of stress shadow influence, the fractures may be affected in width, and in other fracture dimension. To illustrate this, a simple example of five parallel fractures may be considered.

[0098] In this example, the fractures are assumed to have a constant height of 100 ft (30.5 m). The spacing between the fractures is 65 ft (19.8m). Other input parameters are given in **Table 2**.

Young's modulus	6.6×10^{6} psi=4.55e+10Pa
Poisson's ratio	0.35
Rate	12.2 bbl/min=0.032m3/s
Viscosity	300 cp=0.3Pa-s
Height	100 ft=30.5m
Leakoff coefficient	3.9×10^{-2} m/s$^{1/2}$
Stress anisotropy	200 psi=1.4Mpa
Fracture spacing	65 ft=19.8m
No. of perfs per frac	100

Table 2 Input parameters for Case #1

For this simple case, a conventional Perkins-Kern-Nordgren (PKN) model (*see, e.g., Mack, M.G. and Warpinski, N.R., Mechanics of Hydraulic Fracturing. Chapter 6, Reservoir Stimulation, 3rd Ed., eds. Economides, M.J. and Nolte, K.G. John Wiley & Sons* (2000)) for multiple fractures may be modified by incorporating the stress shadow calculation as given from Eq. 6. The increase in closure stress may be approximated by averaging the computed stress from Eq. 6 over the entire fracture. Note that this simplistic PKN model may not simulate the fracture turning due to the stress shadow effect. The results from this simple model may be compared to the results from the UFM model that incorporates point-by-point stress shadow calculation along the entire fracture paths as well as fracture turning.

[0099] Figure 9 shows the simulation results of fracture lengths of the five fractures, computed from both models. Fig. 9 is a graph 900 depicting length (y-axis) versus time (t) of five parallel fractures during injection. Lines 917.1-917.5 are generated from the UFM model. Lines 919.1-919.5 are generated from the simplistic PKN model.

[0100] The fracture geometry and width contour from the UFM model for the five fractures of Figure 9 are shown in Figure 10. Figure 10 is a schematic diagram 1000 depicting fractures 1021.1-1021.5 about a wellbore 1004.

[0101] Fracture 1021.3 is the middle one of the five fractures, and fractures 1021.1 and 1021.5 are the outmost ones. Since fractures 1021.2, 1021.3, and 1021.4 have smaller width than that of the outer ones due to the stress shadow effect, they may have larger flow resistance, receive less flow rate, and have shorter length. Therefore, the stress shadow effects may be fracture width and also fracture length under dynamic conditions.

[0102] The effect of stress shadow on fracture geometry may be influenced by many parameters. To illustrate the effect of some of these parameters, the computed fracture lengths for the cases with varying fracture spacing, perforation friction, and stress anisotropy are shown in **Table 3**.

[0103] Figures 11.1 and 11.2 shows the fracture geometry predicted by the UFM for the case of large perforation friction and the case of large fracture spacing (e.g., about 120 ft (36.6 m)). Figures 11.1 and 11.2 are schematic diagrams 1100.1 and 1100.2 depicting five fractures 1123.1-1123.5 about a wellbore 1104. When the perforation friction is large, a large diversion force that uniformly distributes the flow rate into all perforation clusters may be provided. Consequently, the stress shadow may be overcome and the resulting fracture lengths may become approximately equal as shown in Figure 11.1. When fracture spacing is large, the effect of the stress shadow may dissipate, and fractures may have approximately the same dimensions as shown in Figure 11.2.

Frac	Base case	120 ft spacing (36.6 m)	No. of perfs = 2	Anisotropy = 50 psi (345000Pa)
1	133	113	105	111
2	93	104	104	95
3	83	96	104	99
4	93	104	100	95
5	123	113	109	102

Table 3 Influence of various parameters on fracture geometry

Case #2 Complex fractures

[0104] In an example of Figure 12, the UFM model may be used to simulate a 4-stage hydraulic fracture treatment in a horizontal well in a shale formation. *See, e.g., Cipolla, C., Weng, X., Mack, M., Ganguly, U., Kresse, O., Gu, H., Cohen, C. and Wu, R., Integrating Microseismic Mapping and Complex Fracture Modeling to Characterize Fracture Complexity. Paper SPE 140185 presented at the SPE Hydraulic Fracturing Conference and Exhibition, Woodlands, Texas, USA, January 24–26, 2011,* (hereinafter "Cipolla 2011") the entire contents of which are hereby incorporated by reference in their entirety. The well may be cased and cemented, and each stage pumped through three or four perforation clusters. Each of the four stages may consist of approximately 25,000 bbls (4000 m^3) of fluid and 440,000 lbs (2e+6kg) of proppant. Extensive data may be available on the well, including advanced sonic logs that provide an

estimate of minimum and maximum horizontal stress. Microseismic mapping data may be available for all stages. *See, e.g., Daniels, J., Waters, G., LeCalvez, J., Lassek, J., and Bentley, D., Contacting More of the Barnett Shale Through an Integration of Real-Time Microseismic Monitoring, Petrophysics, and Hydraulic Fracture Design. Paper SPE 110562 presented at the 2007 SPE Annual Technical Conference and Exhibition, Anaheim, California, USA, October 12-14, 2007.* This example is shown in Figure 12. Fig. 12 is a graph depicting microseismic mapping of microseismic events 1223 at various stages about a wellbore 1204.

[0105] The stress anisotropy from the advanced sonic log, indicates a higher stress anisotropy in the toe section of the well compared to the heel. An advanced 3D seismic interpretation may indicate that the dominant natural fracture trend changes from NE-SW in the toe section to NW-SE in heel portion of the lateral. *See, e.g., Rich, J.P. and Ammerman, M., Unconventional Geophysics for Unconventional Plays. Paper SPE 131779 presented at the Unconventional Gas Conference, Pittsburgh, Pennsylvania, USA, February 23-25, 2010*, the entire contents of which is hereby incorporated by reference herein in its entirety.

[0106] Simulation results may be based on the UFM model without incorporating the full stress shadow calculation (*see, e.g., Cipolla 2011*), including shear stress and fracture turning (*see, e.g., Weng 2011*). The simulation may be updated with the full stress model as provided herein. Figures 13.1-13.4 show a plan view of a simulated fracture network 1306 about a wellbore 1304 for all four stages, respectively, and their comparison to the microseismic measurements 1323.1-1323.4, respectively.

[0107] From simulation results in Figures 13.1-13.4, it can be seen that for Stages 1 and 2, the closely spaced fractures did not diverge significantly. This may be because of the high stress anisotropy in the toe section of the wellbore. For Stage 3 and 4, where stress anisotropy is lower, more fracture divergence can be seen as a result of the stress shadow effect.

Case #3 Multi-stage example

[0108] Case #3 is an example showing how stress shadow from previous stages can influence the propagation pattern of hydraulic fracture networks for next treatment stages, resulting in changing of total picture of generated hydraulic fracture network for the four stage treatment

case.

[0109] This case includes four hydraulic fracture treatment stages. The well is cased and cemented. Stages 1 and 2 are pumped through three perforated clusters, and Stages 3 and 4 are pumped through four perforated clusters. The rock fabric is isotropic. The input parameters are listed in Table 4 below. The top view of total hydraulic fracture network without and with accounting for stress shadow from previous stages is shown in Figures 13.1-13.4.

Young's modulus	4.5×10^6 psi=3.1e+10Pa
Poisson's ratio	0.35
Rate	30.9 bpm=0.082m3/s
Viscosity	0.5 cp=0.0005pa-s
Height	330 ft=101m
Pumping time	70 min

Table 4 Input parameters for Case #3

[0110] Figures 14.1-14.4 are schematic diagrams 1400.1-1400.4 depicting a fracture network 1429 at various stages during a fracture operation. Figure 14.1 shows a discrete fracture network (DFN) 1429 before treatment. Figure 14.2 depicts a simulated DFN 1429 after a first treatment stage. The DFN 1429 has propagated hydraulic fractures (HFN) 1431 extending therefrom due to the first treatment stage. Figure 14.3 shows the DFN depicting a simulated HFN 1431.1-1431.4 propagated during four stages, respectively, but without accounting for previous stage effects. Figure 14.4 shows the DFN depicting HFN 1431.1, 1431.2'-1431.4' propagated during four stages, but with accounting for the fractures, stress shadows and HFN from previous stages.

[0111] When stages are generated separately, they may not see each other as indicated in Figure 14.3. When stress shadow and HFN from previous stages are taken into account as in Figure 14.4 the propagation pattern may change. The hydraulic fractures 1431.1 generated for the first stage is the same for both case scenarios as shown in Figures 14.3 and 14.4. The second stage 1431.2 propagation pattern may be influenced by the first stage through stress shadow, as well as through new DFN (including HFN 1431.1 from Stage 1), resulting in the changing of propagation patterns to HFN 1431.2'. The HFN 1431.1' may start to follow HFN 1431.1 created at stage 1 while intercounting it. The third stage 1431.3 may follow a hydraulic fracture created during second stage treatment 1431.2, 1431.2', and may not propagate too far due to stress shadow effect from Stage 2 as indicated by 1431.3 versus 1431.3'. Stage 4 (1431.4) may tend to

turn away from stage three when it could, but may follow HFN 1431.3' from previous stages when encounters it and be depicted as HFN 1431.4' in Figure 14.4.

[0112] A method for computing the stress shadow in a complex hydraulic fracture network is presented. The method may involve an enhanced 2D or 3D Displacement Discontinuity Method with correction for finite fracture height. The method may be used to approximate the interaction between different fracture branches in a complex fracture network for the fundamentally 3D fracture problem. This stress shadow calculation may be incorporated in the UFM, a complex fracture network model. The results for simple cases of two fractures show the fractures can either attract or expel each other depending on their initial relative positions, and compare favorably with an independent 2D non-planar hydraulic fracture model.

[0113] Simulations of multiple parallel fractures from a horizontal well may be used to confirm the behavior of the two outmost fractures that may be more dominant, while the inner fractures have reduced fracture length and width due to the stress shadow effect. This behavior may also depend on other parameters, such as perforation friction and fracture spacing. When fracture spacing is greater than fracture height, the stress shadow effect may diminish and there may be insignificant differences among the multiple fractures. When perforation friction is large, sufficient diversion to distribute the flow equally among the perforation clusters may be provided, and the fracture dimensions may become approximately equal despite the stress shadow effect.

[0114] When complex fractures are created, if the formation has a small stress anisotropy, fracture interaction can lead to dramatic divergence of the fractures where they tend to repel each other. On the other hand, for large stress anisotropy, there may be limited fracture divergence where the stress anisotropy offsets the effect of fracture turning due to the stress shadow, and the fracture may be forced to go in the direction of maximum stress. Regardless of the amount of fracture divergence, the stress shadowing may have an effect on fracture width, which may affect the injection rate distribution into multiple perforation clusters, and overall fracture network footprint and proppant placement.

[0115] Figure 15 is a flow chart depicting a method 1500 of performing a fracture operation at a wellsite, such as the wellsite 100 of Figure 1.1. The wellsite is positioned about a subterranean

formation having a wellbore therethrough and a fracture network therein. The fracture network has natural fractures as shown in Figures 1.1 and 1.2. The method (1500) may involve (1580) performing a stimulation operation by stimulating the wellsite by injection of an injection fluid with proppant into the fracture network to form a hydraulic fracture network. In some cases, the stimulation may be performed at the wellsite or by simulation.

[0116] The method involves (1582) obtaining wellsite data and a mechanical earth model of the subterranean formation. The wellsite data may include any data about the wellsite that may be useful to the simulation, such as natural fracture parameters of the natural fractures, images of the fracture network, etc. The natural fracture parameters may include, for example, density orientation, distribution, and mechanical properties (e.g., coefficients of friction, cohesion, fracture toughness, etc.) The fracture parameters may be obtained from direct observations of borehole imaging logs, estimated from 3D seismic, ant tracking, sonic wave anisotropy, geological layer curvature, microseismic events or images, etc. Examples of techniques for obtaining fracture parameters are provided in PCT/US2012/48871 and US2008/0183451, the entire contents of which are hereby incorporated by reference herein in their entirety.

[0117] Images may be obtained by, for example, observing borehole imaging logs, estimating fracture dimensions from wellbore measurements, obtaining microseismic images, and/or the like. The fracture dimensions may be estimated by evaluating seismic measurements, ant tracking, sonic measurements, geological measurements, and/or the like. Other wellsite data may also be generated from various sources, such as wellsite measurements, historical data, assumptions, etc. Such data may involve, for example, completion, geological structure, petrophysical, geomechanical, log measurement and other forms of data. The mechanical earth model may be obtained using conventional techniques.

[0118] The method (1500) also involves (1584) generating a hydraulic fracture growth pattern over time, such as during the stimulation operation. Figures 16.1-16.4 depict an example of (1584) generating a hydraulic fracture growth pattern. As shown in Figure 16.1, in its initial state, a fracture network 1606.1 with natural fractures 1623 is positioned about a subterranean formation 1602 with a wellbore 1604 therethrough. As proppant is injected into the subterranean formation 1602 from the wellbore 1604, pressure from the proppant creates hydraulic fractures

1691 about the wellbore 1604. The hydraulic fractures 1691 extend into the subterranean formation along L_1 and L_2 (Figure 16.2), and encounter other fractures in the fracture network 1606.1 over time as indicated in Figures 16.2-16.3. The points of contact with the other fractures are intersections 1625.

[0119] The generating (1584) may involve (1586) extending hydraulic fractures from the wellbore and into the fracture network of the subterranean formation to form a hydraulic fracture network including the natural fractures and the hydraulic fractures as shown in Figure 16.2. The fracture growth pattern is based on the natural fracture parameters and a minimum stress and a maximum stress on the subterranean formation. The generating may also involve (1588) determining hydraulic fracture parameters (e.g., pressure p, width w, flow rate q, etc.) of the hydraulic fractures, (1590) determining transport parameters for the proppant passing through the hydraulic fracture network, and (1592) determining fracture dimensions (e.g., height) of the hydraulic fractures from, for example, the determined hydraulic fracture parameters, the determined transport parameters and the mechanical earth model. The hydraulic fracture parameters may be determined after the extending. The determining (1592) may also be performed by from the proppant transport parameters, wellsite parameters and other items.

[0120] The generating (1584) may involve modeling rock properties based on a mechanical earth model as described, for example, in *Koutsabeloulis and Zhang, 3D Reservoir Geomechanics Modeling in Oil/Gas Field Production, SPE Paper 126095, 2009 SPE Saudi Arabia Section Technical Symposium and Exhibition held in Al Khobar, Saudi Arabia, 9-11 May, 2009*. The generating may also involve modeling the fracture operation by using the wellsite data, fracture parameters and/or images as inputs modeling software, such as UFM, to generate successive images of induced hydraulic fractures in the fracture network.

[0121] The method (1500) also involves (1594) performing stress shadowing on the hydraulic fractures to determine stress interference between the hydraulic fractures (or with other fractures), and (1598) repeating the generating (1584) based on the stress shadowing and/or the determined stress interference between the hydraulic fractures. The repeating may be performed to account for fracture interference that may affect fracture growth. Stress shadowing may involve performing, for example, a 2D or 3D DDM for each of the hydraulic fractures and

updating the fracture growth pattern over time. The fracture growth pattern may propagate normal to a local principal stress direction according to stress shadowing. The fracture growth pattern may involve influences of the natural and hydraulic fractures over the fracture network (see Fig. 16.3).

[0122] Stress shadowing may be performed for multiple wellbores of the wellsite. The stress shadowing from the various wellbores may be combined to determine the interaction of fractures as determined from each of the wellbores. The generating may be repeated for each of the stress shadowings performed for one or more of the multiple wellbores. The generating may also be repeated for stress shadowing performed where stimulation is provided from multiple wellbores. Multiple simulations may also be performed on the same wellbore with various combinations of data, and compared as desired. Historical or other data may also be input into the generating to provide multiple sources of information for consideration in the ultimate results.

[0123] The method also involves (1596) determining crossing behavior between the hydraulic fractures and an encountered fracture if the hydraulic fracture encounters another fracture, and (1598) repeating the generating (1584) based on the crossing behavior if the hydraulic fracture encounters a fracture (see, e.g., Figure 16.3). Crossing behavior may be determined using, for example, the techniques of PCT/US2012/059774, the entire contents of which is hereby incorporated herein in its entirety.

[0124] The determining crossing behavior may involve performing stress shadowing. Depending on downhole conditions, the fracture growth pattern may be unaltered or altered when the hydraulic fracture encounters the fracture. When a fracture pressure is greater than a stress acting on the encountered fracture, the fracture growth pattern may propagate along the encountered fracture. The fracture growth pattern may continue propagation along the encountered fracture until the end of the natural fracture is reached. The fracture growth pattern may change direction at the end of the natural fracture, with the fracture growth pattern extending in a direction normal to a minimum stress at the end of the natural fracture as shown in Figure 16.4. As shown in Figure 16.4, the hydraulic fracture extends on a new path 1627 according to the local stresses σ_1 and σ_2.

[0125] Optionally, the method (1500) may also involve (1599) validating the fracture growth

pattern. The validation may be performed by comparing the resulting growth pattern with other data, such as microseismic images as shown, for example, in Figures 7.1 and 7.2.

[0126] The method may be performed in any order and repeated as desired. For example, the generating (1584) - (1599) may be repeated over time, for example, by iteration as the fracture network changes. The generating (1584) may be performed to update the iterated simulation performed during the generating to account for the interaction and effects of multiple fractures as the fracture network is stimulated over time.

[0127] The method 1500 may be used for a variety of wellsite conditions having perforations and fractures, such as fractures 811.1-811.3 as depicted in Figure 8. In the example of Figure 8, the fractures 811.1-811.3 may be positioned at about the same depth in the formation. In some cases, the fractures may be at different depths as shown, for example, in Figures 18-20.

[0128] Figures 18-20 show various example schematic plots 1800, 1900, 2000 of parallel transverse fractures 1811.1, 1811.2 propagating simultaneously from multiple perforation clusters 1815.1, 1815.2, respectively, about an inclined wellbore 1804 in formation 1802. Each of the fractures 1811.1, 1811.2 traverses strata 1817.1, 1817.2, 1817.3, 1817.4, 1817.5, 1817.6 at various depths D1-D6, respectively, along formation 1802. The formation 1802 may have one or more strata of various makeup, such as shale, sand, rock, etc. The formation 1802 has an overall stress σf, and each strata 1817.1-1817.6 has a corresponding stress $\sigma f1$-$\sigma f6$, respectively.

[0129] Figures 18 and 19 may be generating using the stress-shadowing as described above. In the example of Figure 18, the fracture 1811.1 extends through strata 1817.2-1817.4 and fracture 1811.2 extends through strata 1817.3-1817.5. In the example of Figure 19, the fracture 1811.2' extends through strata 1817.2-1817.5. As shown by Figure 19, the fractures may have a given vertical length and extend a given distance through one or more strata and receive the corresponding stress effects therefrom.

[0130] In the example of Fig. 19, the fractures 1811.1, 1811.2' are taken without considering the effects of stress shadowing. In this case, height growth of the fractures 1811.1 and 1811.2' is influenced by the vertical in-situ stress distribution of the stresses σf of the corresponding strata around the fractures. Fracture 1811.1 has a vertical length L1 above the perforation cluster

1815.1 and a vertical length L2 below the perforation cluster 1815.1. Fracture 1811.2' has a vertical length L3 above the perforation cluster 1815.2 and a vertical length L4 below the perforation cluster 1815.2.

[0131] Figure 20 may be generated by stress shadowing using 3D DDM as described above. In the example of Figure 20, the fracture 1811.1' extends through strata 1817.1-1817.4 and fracture 1811.2'' extends through strata 1817.3-1817.6. Fig. 20 shows a cross section of the fractures of Figure 19 once the effect of vertical stress shadowing is taken into consideration. The fracture 1811.1 grows more upward and fracture 1811.2 grows more downward due to the stress shadowing.

[0132] In this case, height growth of the fractures is influenced by the vertical in-situ stress distribution plus the stress shadow of the adjacent fractures. Fracture 1811.1' has an extended vertical length L1' above the perforation cluster 1815.1 and a reduced vertical length L2' below the perforation cluster 1815.1. Fracture 1811.2'' has a reduced vertical length L3' above the perforation cluster 1815.2 and an extended vertical length L4' below the perforation cluster 1815.2. The growth shown in Figure 20 reflects the divergent growth due to interaction of the fractures as schematically depicted by the arrows of Figure 18.

[0133] As in Figures 19-20, where fractures are at different depths and subject to different stresses, the height growth of the fractures may vary depending on the relative fracture height. The fractures are initiated from different formations, and the presence of the adjacent fracture can help prevent one fracture from growing into the layer of strata occupied by another fracture due to the vertical stress shadowing effect.

[0134] The stress shadowing described herein may take into consideration interaction between the fractures at the same or different depths. For example in Figure 8, the middle fracture may be compressed by the fractures on either side thereof and become smaller and narrower as described with respect to Figure 10. The UFM model provided herein may be used to describe such interaction. In another example, as shown in Figures 18-20, the two fractures may compress each other and drive the fractures apart. In this example, fracture 1811.1 extends upward and the fracture on the right grows downward due to the slant of the wellbore.

[0135] Figure 21 depicts another version of the method 2100 that may take into consideration the effects of the fractures at various depths. The method 2100 may take into consideration stress interference between hydraulic fractures to evaluate the height growth of each fracture whether at the same or different depths. The method 2100 may be used to perform a fracture operation at a wellsite having a wellbore with a fracture network thereabout as shown, for example, in Figures 18-20. In this version, the method 2100 may be performed according to part or all of the method 1500 as previously described with respect to Figure 15, except with an additional stress shadowing 2195, a modified determining 1596', and a modified repeating 1598'.

[0136] The additional stress shadowing 2195 may be performed based on vertical growth of the hydraulic fractures to take into consideration the effects of hydraulic fractures at different depths. The additional stress shadowing 2195 may be performed using 3D DDM when the fractures are at different depths (see, e.g., Figs. 18-20). The additional stress shadowing 2195 may be performed after the performing 1594 and before the modified determining 1596'. In some cases, the additional stress shadowing 2195 may be performed simultaneously with the performing stress shadowing 1594. For example, where the performing 1594 is done using 3D DDM, the depth may be taken into consideration without the additional stress shadowing 2195. In some cases, the performing 1594 may be done using another technique, such as 2D DDM, and the depth of the fractures may be taken into consideration with the additional stress shadowing 2195 using 3D DDM. The 3D DDM may take into consideration the influence of adjacent fractures and associated vertical stresses, and generate an adjusted vertical growth and/or length.

[0137] The determining 1596' and the repeating 1598' may be modified to take into consideration the additional 2195 stress shadowing, if performed. The modified determining 1596' involves, determining the crossing behavior between the hydraulic fracture and the encountered fracture based on the performing 1594 and the additional stress shadowing 2195. The modified repeating 1598' involves repeating the fracture growth pattern based on the 1594 determining stress interference, the 2195 additional stress shadowing, and the 1596' determining crossing behavior.

[0138] An additional adjusting 2197 may be performed based on the stress shadowing 1594 and/or 2195. For example, the fracture growth may be offset by adjusting at least one

stimulation parameter, such as pumping pressures, fluid viscosity, etc., during injection (or fracturing). The fracture growth may be simulated using the UFM model modified for the adjusted pumping parameters.

[0139] One or more portions of the method, such as the performing the stimulation operation 1580 may be repeated based on part or all of 1594-1599. For example, based on the stress shadowing 1594 and/or 2195, and/or the resulting fracture growth, the stimulation may be adjusted to achieve the desired fracture growth (see, e.g., Figure 20). The stimulating may be modified, for example, by adjusting pumping pressures, fluid viscosities and/or other injection parameters to achieve the desired wellsite operation and/or a desired fracture growth.

[0140] Various combinations of part or all of the methods of Figures 15 and/or 21 may be performed in various orders.

[0141] Although the present disclosure has been described with reference to exemplary embodiments and implementations thereof, the present disclosure is not to be limited by or to such exemplary embodiments and/or implementations. Rather, the systems and methods of the present disclosure are susceptible to various modifications, variations and/or enhancements without departing from the spirit or scope of the present disclosure. Accordingly, the present disclosure expressly encompasses all such modifications, variations and enhancements within its scope.

[0142] It should be noted that in the development of any such actual embodiment, or numerous implementation, specific decisions may be made to achieve the developer's specific goals, such as compliance with system related and business related constraints, which will vary from one implementation to another. Moreover, it will be appreciated that such a development effort might be complex and time consuming but would nevertheless be a routine undertaking for those of ordinary skill in the art having the benefit of this disclosure. In addition, the embodiments used/disclosed herein can also include some components other than those cited.

[0143] In the description, each numerical value should be read once as modified by the term "about" (unless already expressly so modified), and then read again as not so modified unless otherwise indicated in context. Also, in the description, it should be understood that any range

listed or described as being useful, suitable, or the like, is intended that values within the range, including the end points, is to be considered as having been stated. For example, "a range of from 1 to 10" is to be read as indicating possible numbers along the continuum between about 1 and about 10. Thus, even if specific data points within the range, or even no data points within the range, are explicitly identified or refer to a few specific ones, it is to be understood that inventors appreciate and understand that any and all data points within the range are to be considered to have been specified, and that inventors possessed knowledge of the entire range and all points within the range.

[0144] The statements made herein merely provide information related to the present disclosure and may not constitute prior art, and may describe some embodiments illustrating the invention. All references cited herein are incorporated by reference into the current application in their entirety.

[0145] Although a few example embodiments have been described in detail above, those skilled in the art will readily appreciate that many modifications are possible in the example embodiments without materially departing from the system and method for performing wellbore stimulation operations. Accordingly, all such modifications are intended to be included within the scope of this disclosure as defined in the following claims. In the claims, means-plus-function clauses are intended to cover the structures described herein as performing the recited function and a structural equivalents and equivalent structures. Thus, although a nail and a screw may not be structural equivalents in that a nail employs a cylindrical surface to secure wooden parts together, whereas a screw employs a helical surface, in the environment of fastening wooden parts, a nail and a screw may be equivalent structures. It is the express intention of the applicant not to invoke 35 U.S.C. § 112, paragraph 6 for any limitations of any of the claims herein, except for those in which the claim expressly uses the words 'means for' together with an associated function.

CLAIMS

What is claimed is:

1. A method of performing a fracture operation at a wellsite, the wellsite positioned about a subterranean formation having a wellbore therethrough and a fracture network therein, the fracture network comprising natural fractures, the wellsite stimulated by injection of an injection fluid with proppant into the fracture network, the method comprising:

obtaining wellsite data comprising natural fracture parameters of the natural fractures and obtaining a mechanical earth model of the subterranean formation;

generating a hydraulic fracture growth pattern for the fracture network over time, the generating comprising:

extending hydraulic fractures from the wellbore and into the fracture network of the subterranean formation to form a hydraulic fracture network comprising the natural fractures and the hydraulic fractures;

determining hydraulic fracture parameters of the hydraulic fractures after the extending;

determining transport parameters for the proppant passing through the hydraulic fracture network; and

determining fracture dimensions of the hydraulic fractures from the determined hydraulic fracture parameters, the determined transport parameters and the mechanical earth model; and

performing stress shadowing on the hydraulic fractures to determine stress interference between the hydraulic fractures at different depths; and

repeating the generating based on the determined stress interference.

2. The method of Claim 1, wherein the performing stress shadowing comprises performing a three dimensional displacement discontinuity method.

3. The method of Claim 1, wherein the performing stress shadowing comprises performing a first stress shadowing to determine interference between the hydraulic fractures and performing a second stress shadowing to determine interference between the hydraulic fractures at different depths.

4. The method of Claim 1, wherein the performing stress shadowing comprises performing a two dimensional displacement discontinuity method and performing a three dimensional displacement discontinuity method.

5. The method of Claim 1, further comprising if the hydraulic fractures encounter another fracture, determining crossing behavior at the encountered another fracture, and wherein the repeating comprises repeating the generating based on the determined stress interference and the crossing behavior.

6. The method of Claim 5, wherein the hydraulic fracture growth pattern is one of unaltered and altered by the crossing behavior.

7. The method of Claim 5, wherein a fracture pressure of the hydraulic fracture network is greater than a stress acting on the encountered fracture and wherein the fracture growth pattern propagates along the encountered fracture.

8. The method of Claim 1, wherein the fracture growth pattern continues to propagate along the encountered fracture until an end of the natural fracture is reached.

9. The method of Claim 1, wherein the fracture growth pattern changes direction at the end of the natural fracture, the fracture growth pattern extending in a direction normal to a minimum stress at the end of the natural fracture.

10. The method of Claim 1, wherein the fracture growth pattern propagates normal to a local principal stress according to the stress shadowing.

11. The method of Claim 1, wherein the stress shadowing comprises performing displacement discontinuity for each of the hydraulic fractures.

12. The method of Claim 1, wherein the stress shadowing comprises performing the stress shadowing about multiple wellbores of a wellsite and repeating the generating using the stress shadowing performed on the multiple wellbores.

13. The method of Claim 1, wherein the stress shadowing comprises performing the stress shadowing at multiple stimulation stages in the wellbore.

14. The method of Claim 1, further comprising validating the fracture growth pattern by comparing the fracture growth pattern with at least one simulation of stimulation of the fracture network.

15. The method of Claim 1, wherein the extending comprises extending the hydraulic fractures along the hydraulic fracture growth pattern based on the natural fracture parameters and

a minimum stress and a maximum stress on the subterranean formation.

16. The method of Claim 1, wherein the determining fracture dimensions comprises one of evaluating seismic measurements, ant tracking, sonic measurements, geological measurements and combinations thereof.

17. The method of Claim 1, wherein the wellsite data further comprises at least one of geological, petrophysical, geomechanical, log measurements, completion, historical and combinations thereof.

18. The method of Claim 1, wherein the natural fracture parameters are generated by one of observing borehole imaging logs, estimating fracture dimensions from wellbore measurements, obtaining microseismic images, and combinations thereof.

19. A method of performing a fracture operation at a wellsite, the wellsite positioned about a subterranean formation having a wellbore therethrough and a fracture network therein, the fracture network comprising natural fractures, the wellsite stimulated by injection of an injection fluid with proppant into the fracture network, the method comprising:

obtaining wellsite data comprising natural fracture parameters of the natural fractures and obtaining a mechanical earth model of the subterranean formation;

generating a hydraulic fracture growth pattern for the fracture network over time, the generating comprising:

extending hydraulic fractures from the wellbore and into the fracture network of the subterranean formation to form a hydraulic fracture network comprising the natural fractures and the hydraulic fractures;

determining hydraulic fracture parameters of the hydraulic fractures after the extending;

determining transport parameters for the proppant passing through the hydraulic fracture network; and

determining fracture dimensions of the hydraulic fractures from the determined hydraulic fracture parameters, the determined transport parameters and the mechanical earth model; and

performing stress shadowing on the hydraulic fractures to determine stress interference between the hydraulic fractures;

performing an additional stress shadowing on the hydraulic fractures to determine stress interference between the hydraulic fractures at different depths;

if the hydraulic fracture encounters another fracture, determining crossing behavior between the hydraulic fractures and an encountered fracture based on the determined stress interference; and

repeating the generating based on the determined stress interference and the crossing behavior.

20. The method of Claim 19, further comprising validating the fracture growth pattern.

21. A method of performing a fracture operation at a wellsite, the wellsite positioned about a subterranean formation having a wellbore therethrough and a fracture network therein, the fracture network comprising natural fractures, the method comprising:

stimulating the wellsite by injection of an injection fluid with proppant into the fracture network;

obtaining wellsite data comprising natural fracture parameters of the natural fractures and obtaining a mechanical earth model of the subterranean formation;

generating a hydraulic fracture growth pattern for the fracture network over time, the generating comprising:

extending hydraulic fractures from the wellbore and into the fracture network of the subterranean formation to form a hydraulic fracture network comprising the natural fractures and the hydraulic fractures;

determining hydraulic fracture parameters of the hydraulic fractures after the extending;

determining transport parameters for the proppant passing through the hydraulic fracture network; and

determining fracture dimensions of the hydraulic fractures from the determined hydraulic fracture parameters, the determined transport parameters and the mechanical earth model; and

performing stress shadowing on the hydraulic fractures to determine stress interference between the hydraulic fractures at different depths;

repeating the generating based on the determined stress interference; and

adjusting the stimulating based on the stress shadowing.

22. The method of Claim 20, further comprising validating the hydraulic fracture growth pattern.

23. The method of Claim 20, further comprising if the hydraulic fractures encounters another fracture, determining crossing behavior between the hydraulic fractures and the encountered another fracture, and wherein the repeating comprises repeating the generating based on the determined stress interference and the crossing behavior.

24. The method of Claim 21, wherein the adjusting comprises changing at least one stimulation parameter comprising pumping rate and fluid viscosity.

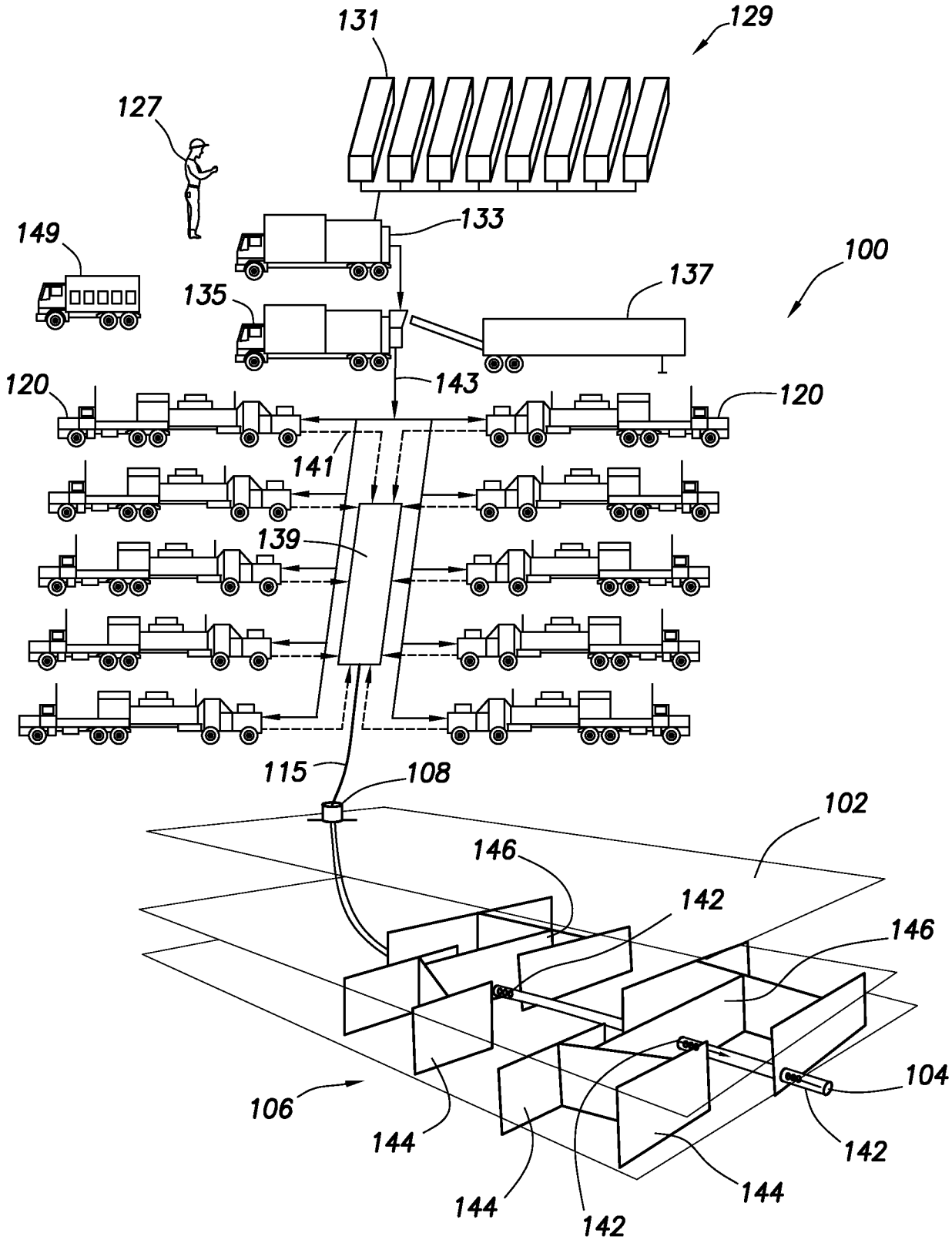
131
129
127
133
149
100
135
137
120
143
120
141
139
115
108
102
146
142
146
104
106
144
142
144
144
142

FIG. 1.1

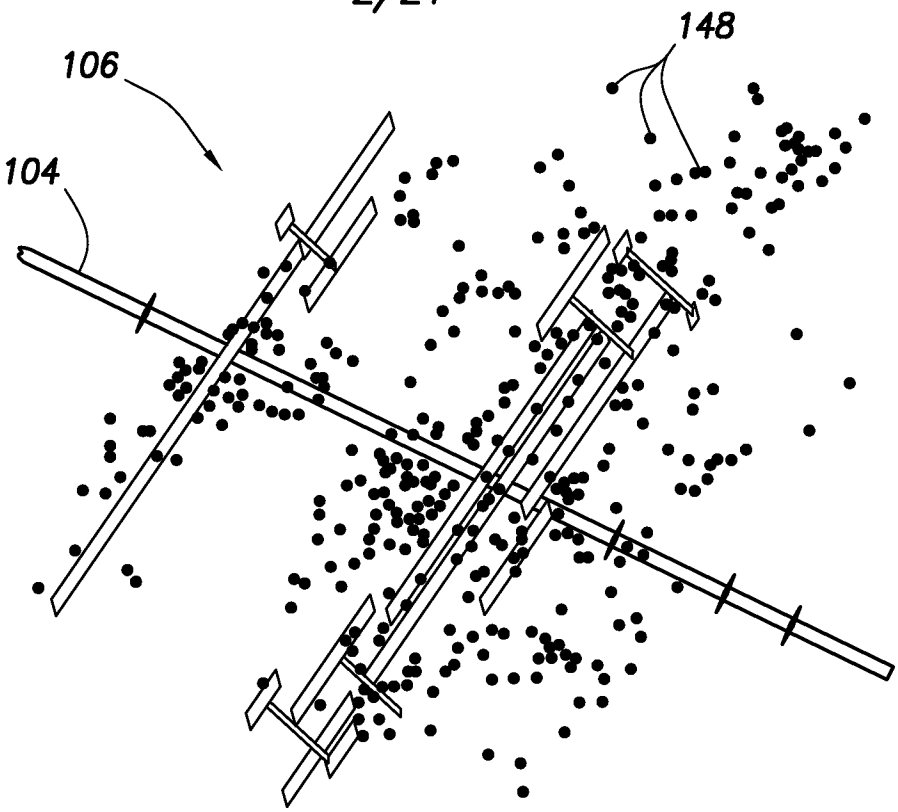

FIG. 1.2

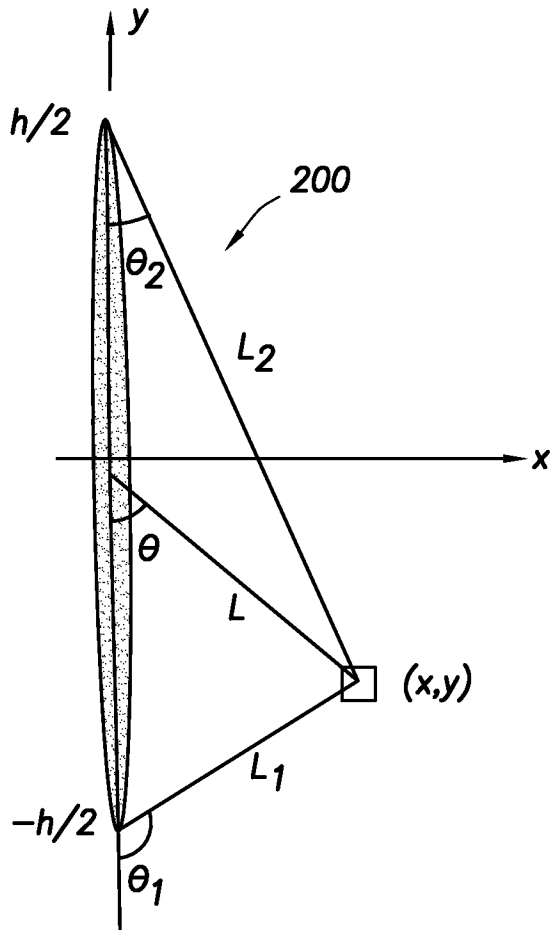

FIG. 2

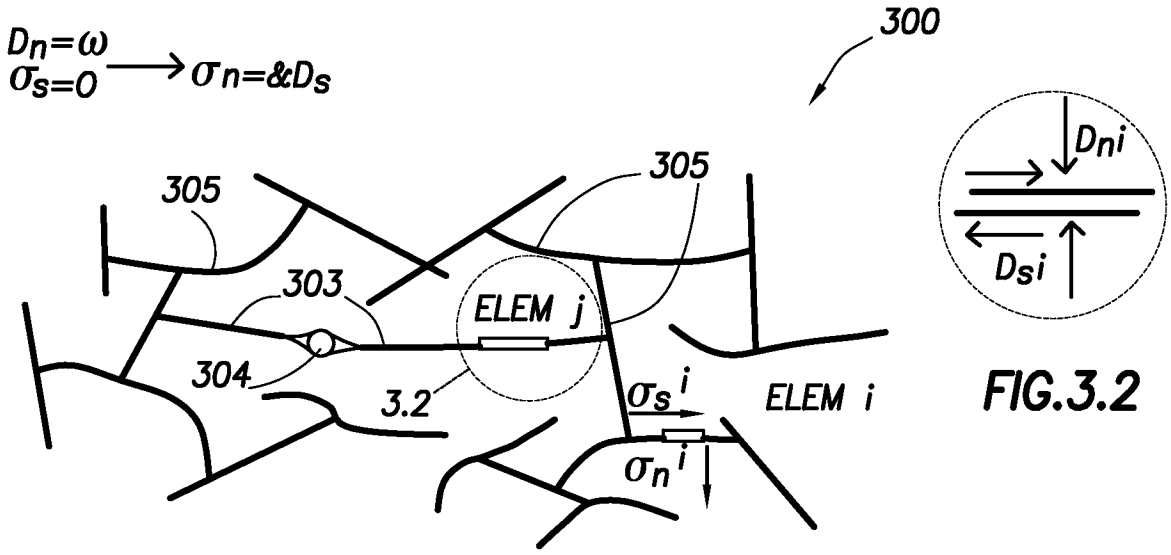

FIG.3.2

FIG.3.1

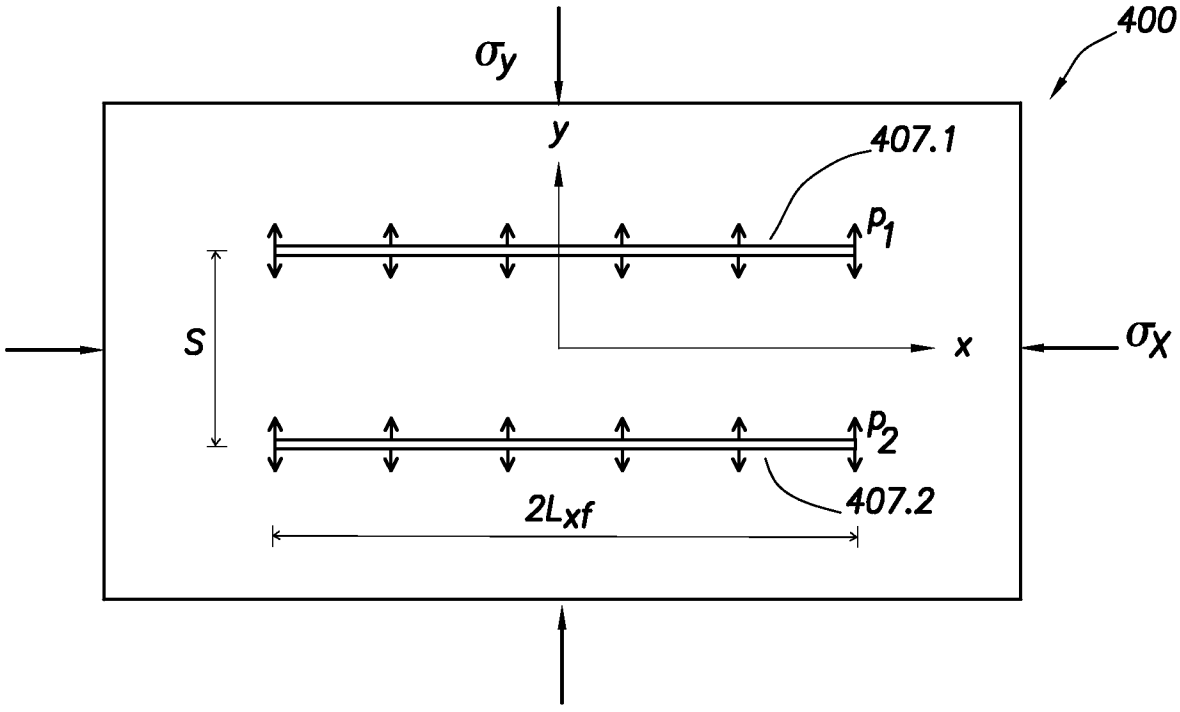

FIG.4

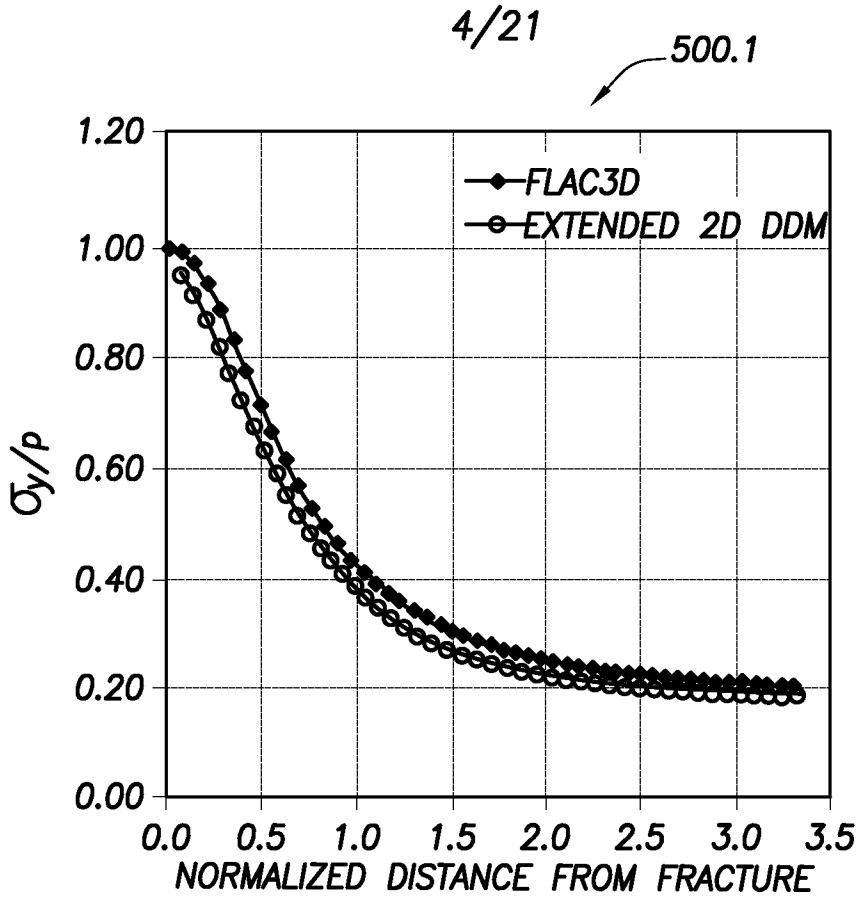
500.1
FLAC3D
EXTENDED 2D DDM
1.20
1.00
0.80
0.60
0.40
0.20
0.00
σy/p
0.0 0.5 1.0 1.5 2.0 2.5 3.0 3.5
NORMALIZED DISTANCE FROM FRACTURE

FIG.5.1

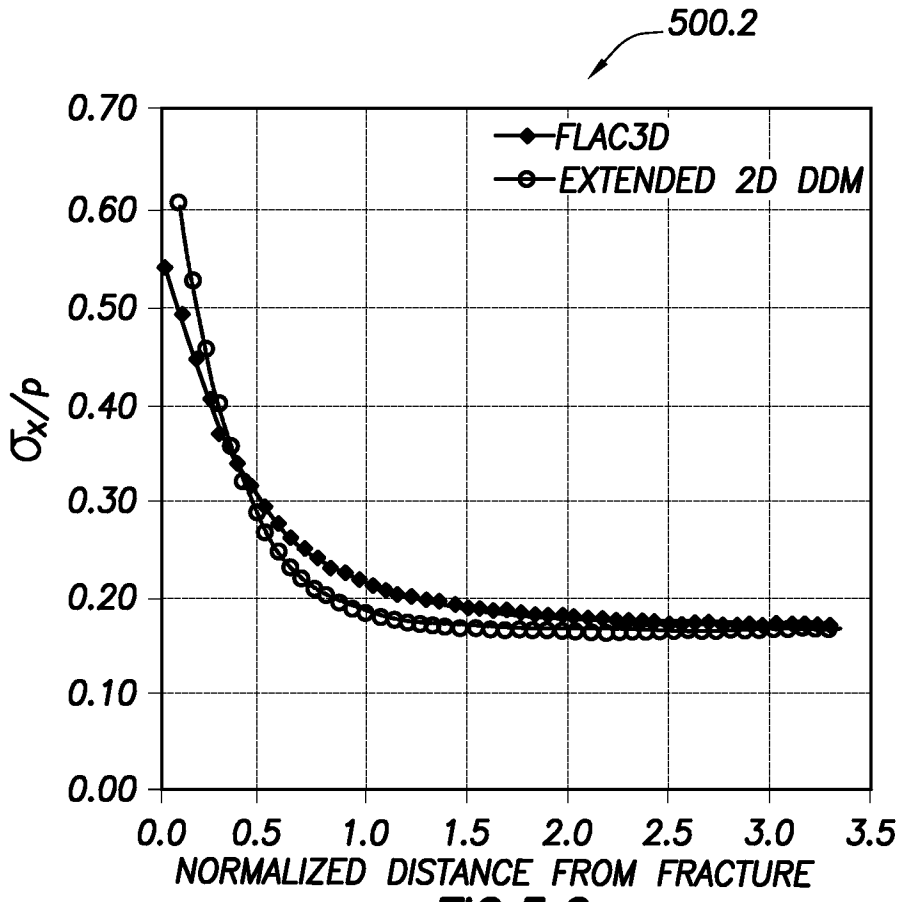
500.2
FLAC3D
EXTENDED 2D DDM
0.70
0.60
0.50
0.40
0.30
0.20
0.10
0.00
σx/p
0.0 0.5 1.0 1.5 2.0 2.5 3.0 3.5
NORMALIZED DISTANCE FROM FRACTURE

FIG.5.2

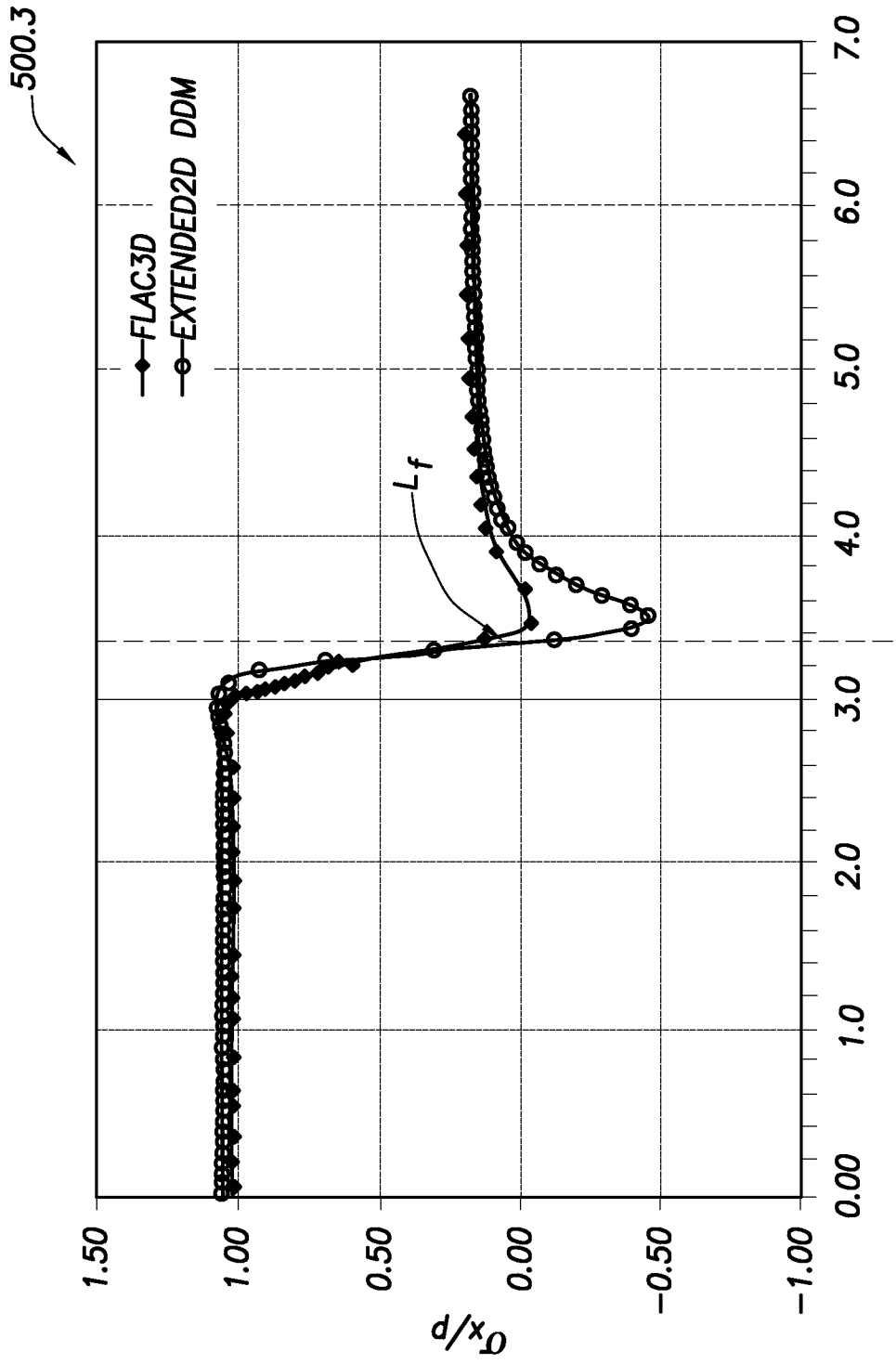
500.3
FLAC3D
EXTENDED2D DDM
L_f
σ_x/p
x/h
1.50
1.00
0.50
0.00
−0.50
−1.00
0.00
1.0
2.0
3.0
4.0
5.0
6.0
7.0

FIG.5.3

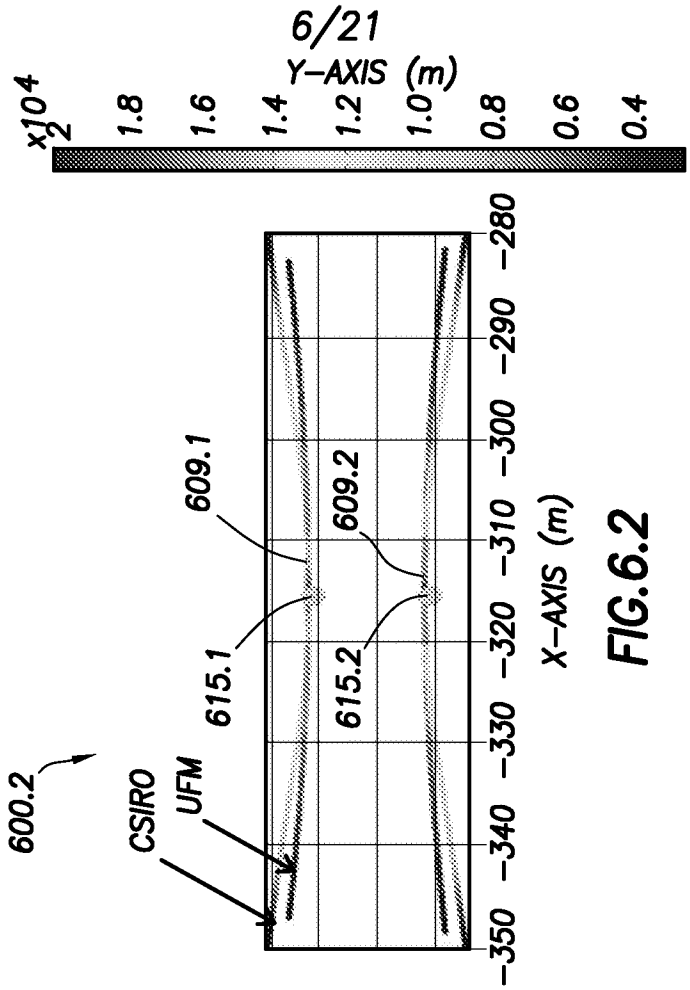
x10^4
2
1.8
1.6
1.4
1.2
1.0
0.8
0.6
0.4
Y-AXIS (m)
600.2
CSIRO
UFM
609.1
609.2
615.1
615.2
-280
-290
-300
-310
-320
-330
-340
-350
X-AXIS (m)

FIG.6.2

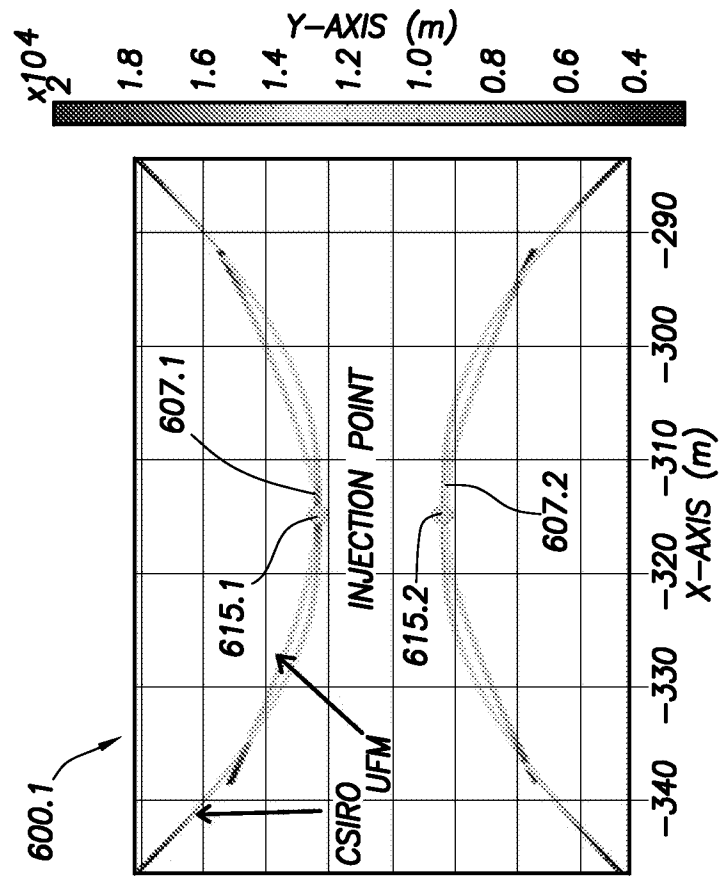
x10^4
2
1.8
1.6
1.4
1.2
1.0
0.8
0.6
0.4
Y-AXIS (m)
600.1
CSIRO
UFM
607.1
607.2
615.1
615.2
INJECTION POINT
-290
-300
-310
-320
-330
-340
X-AXIS (m)

FIG.6.1

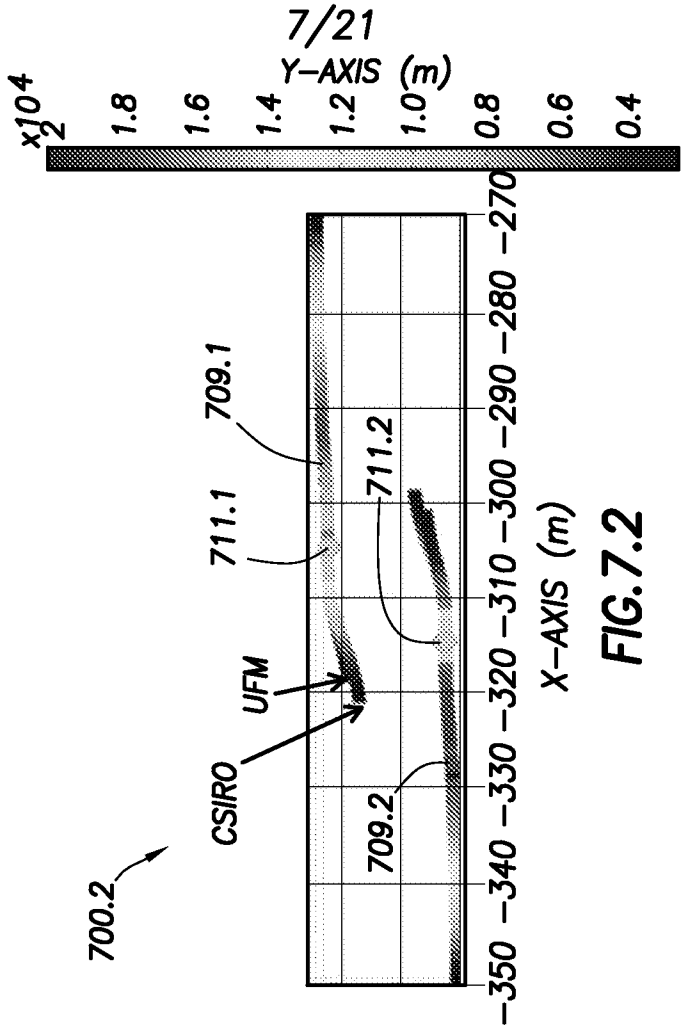
Y-AXIS (m)
x10^4
2
1.8
1.6
1.4
1.2
1.0
0.8
0.6
0.4
709.1
711.1
711.2
UFM
CSIRO
709.2
700.2
-270
-280
-290
-300
-310
-320
-330
-340
-350
X-AXIS (m)

FIG.7.2

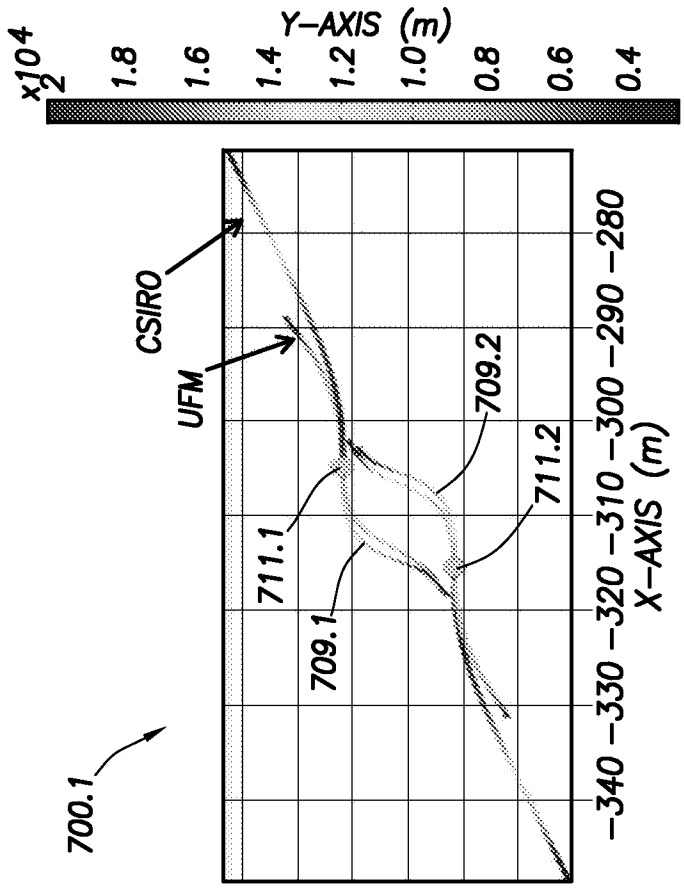
Y-AXIS (m)
x10^4
2
1.8
1.6
1.4
1.2
1.0
0.8
0.6
0.4
CSIRO
UFM
709.2
711.2
711.1
709.1
700.1
-280
-290
-300
-310
-320
-330
-340
X-AXIS (m)

FIG.7.1

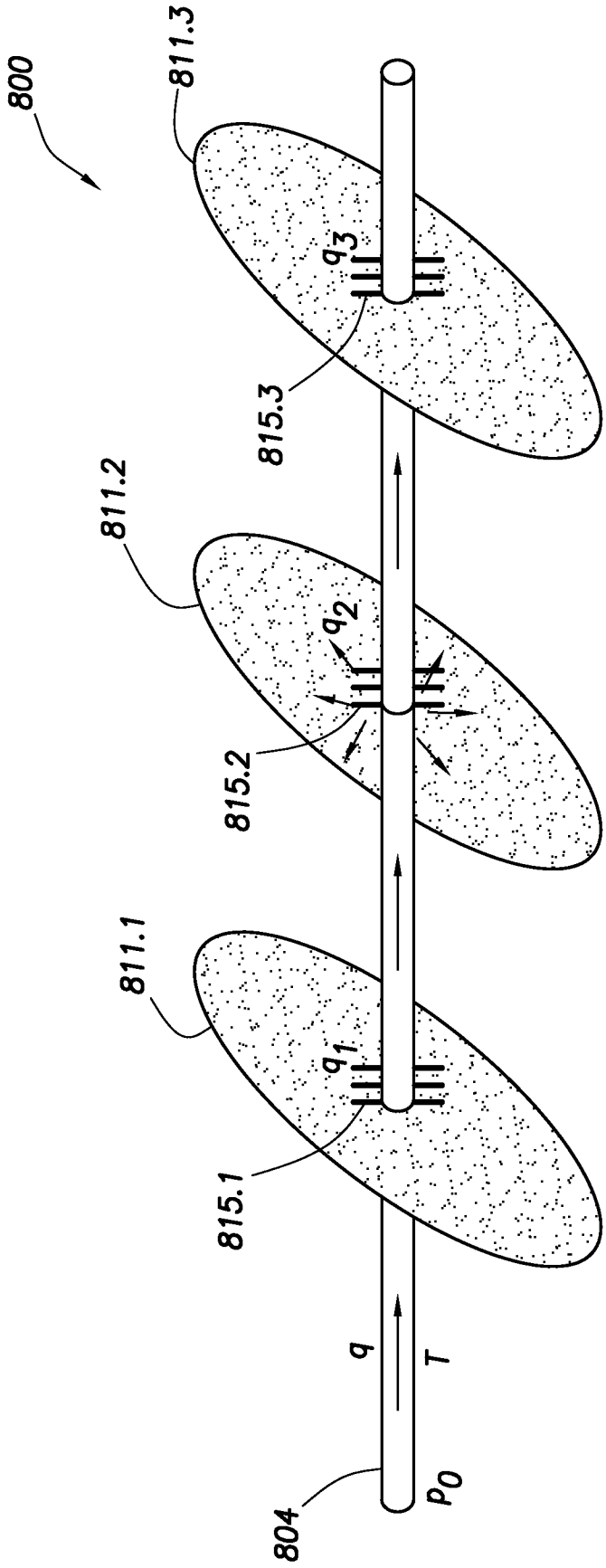

FIG.8

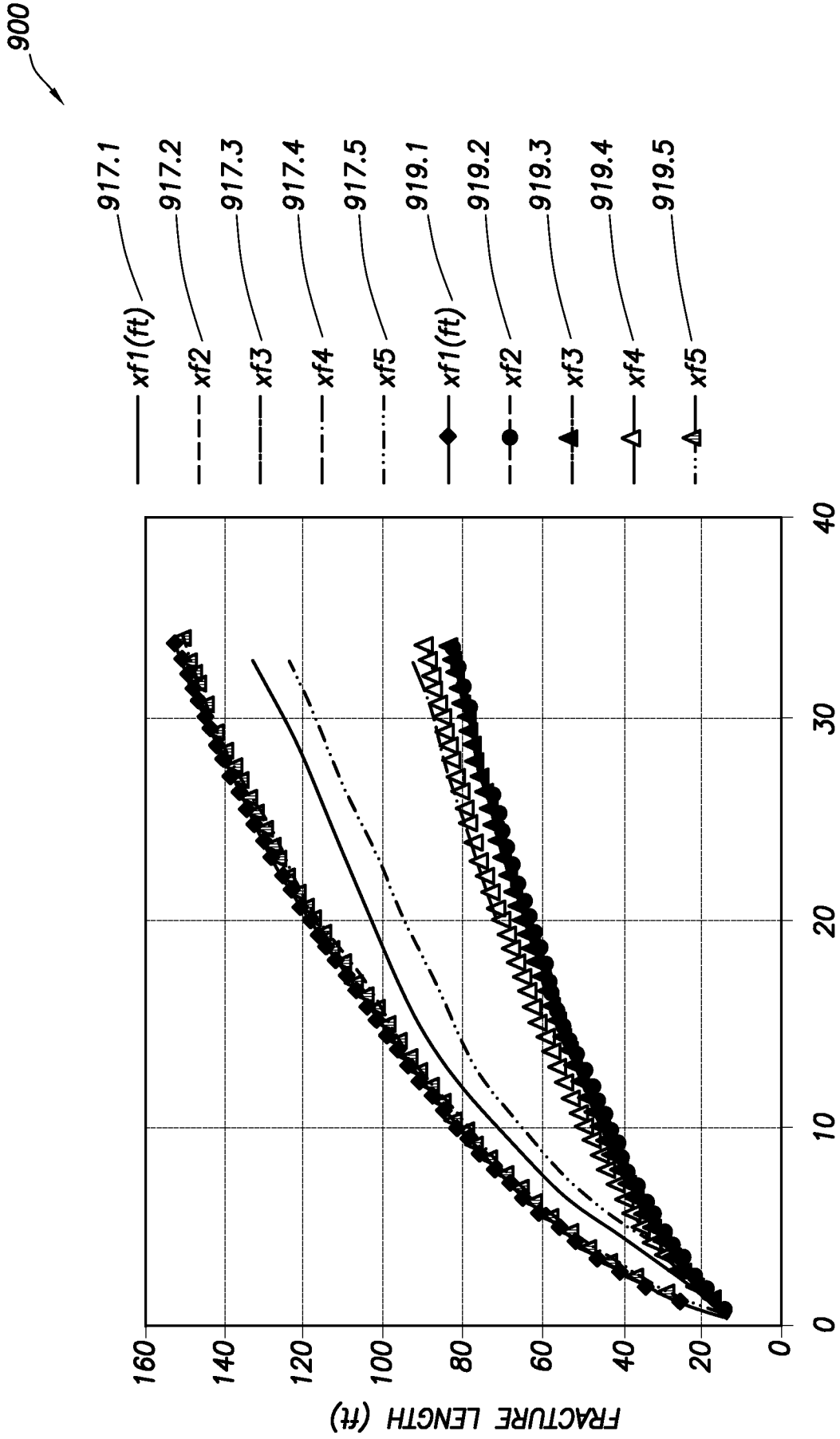
900
917.1
xf1(ft)
917.2
xf2
917.3
xf3
917.4
xf4
917.5
xf5
919.1
xf1(ft)
919.2
xf2
919.3
xf3
919.4
xf4
919.5
xf5
FRACTURE LENGTH (ft)
160
140
120
100
80
60
40
20
0
0
10
20
30
40
TIME (min)

FIG.9

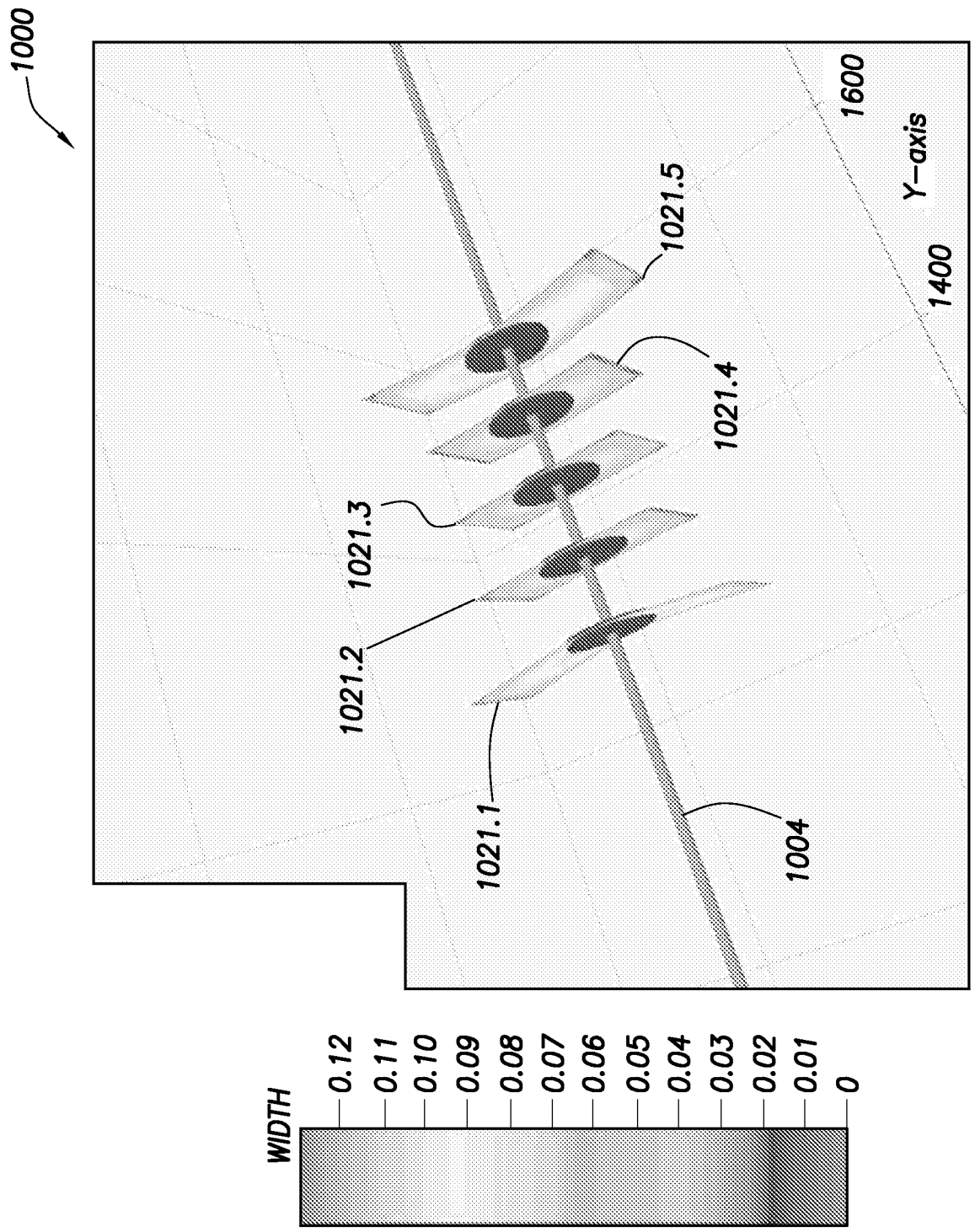
1000
1600
Y-axis
1400
1021.5
1021.4
1021.3
1021.2
1021.1
1004
WIDTH
0.12
0.11
0.10
0.09
0.08
0.07
0.06
0.05
0.04
0.03
0.02
0.01
0

FIG. 10

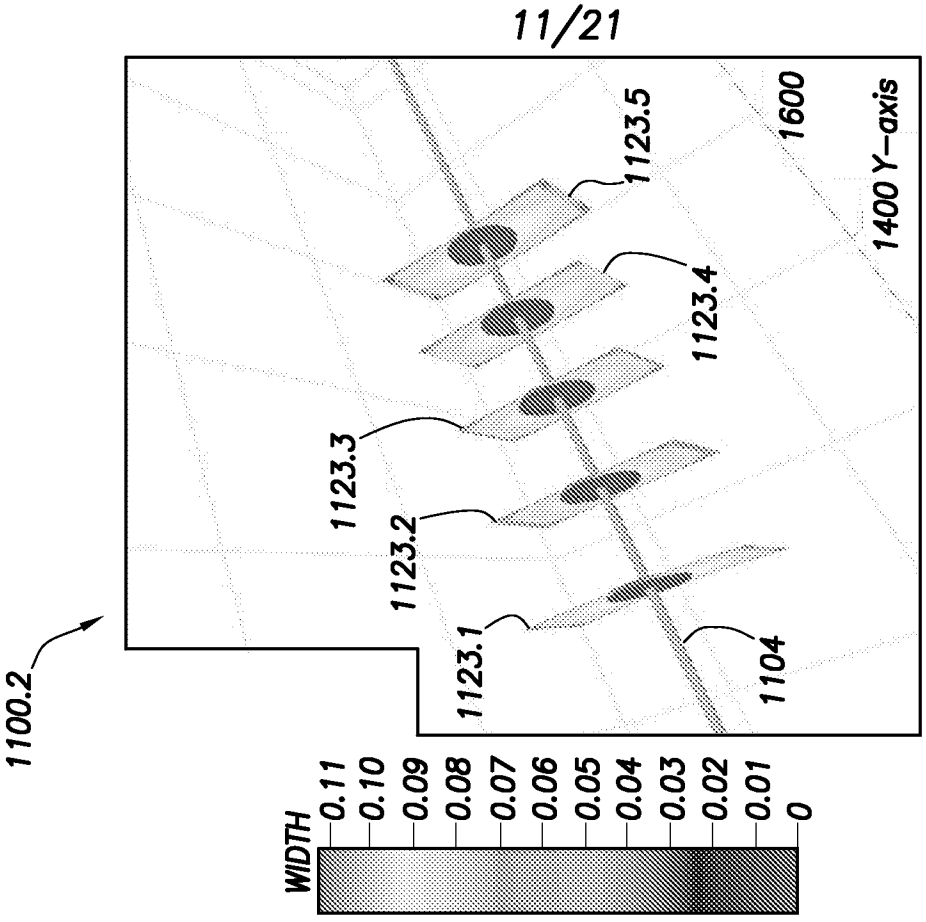

FIG.11.2

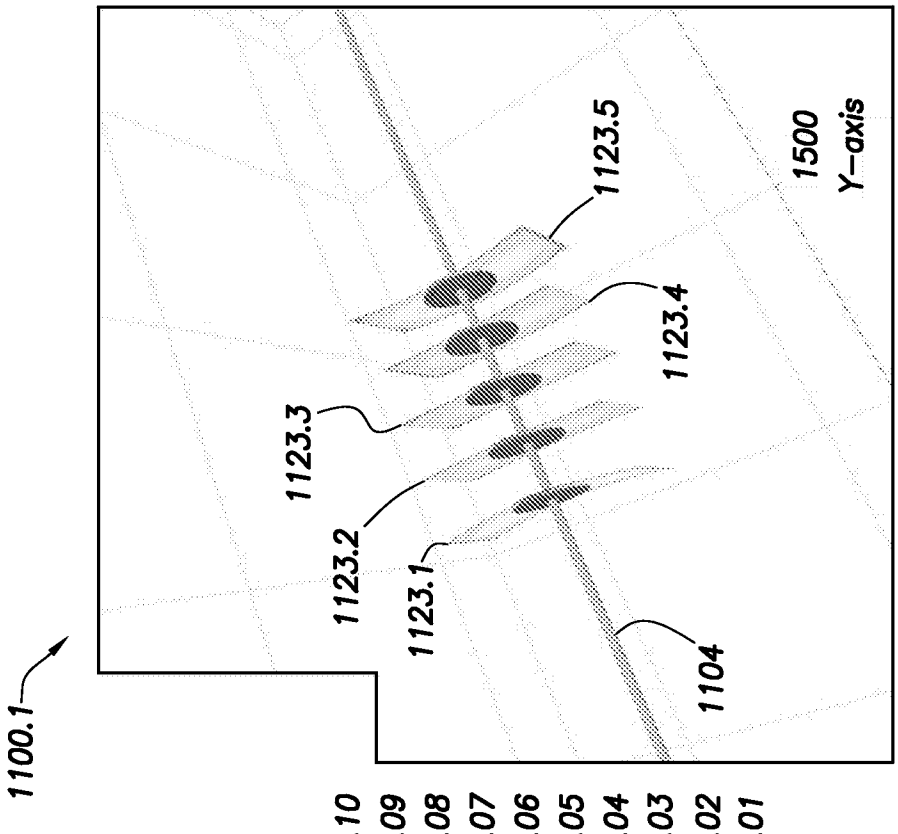

FIG.11.1

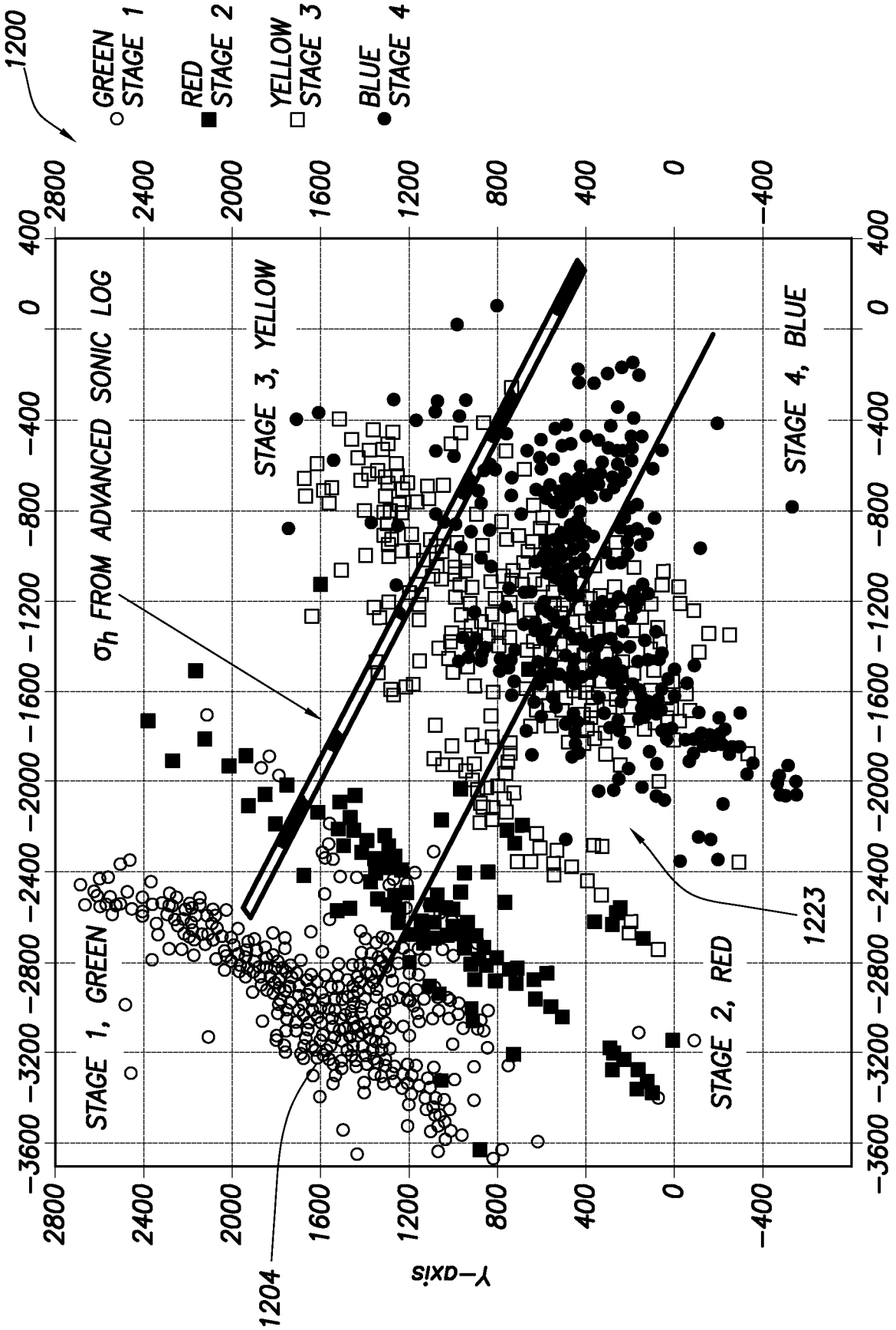
1200
GREEN
STAGE 1
RED
STAGE 2
YELLOW
STAGE 3
BLUE
STAGE 4
σh FROM ADVANCED SONIC LOG
STAGE 1, GREEN
STAGE 3, YELLOW
STAGE 4, BLUE
STAGE 2, RED
1204
1223
Y-axis
X-axis

FIG.12

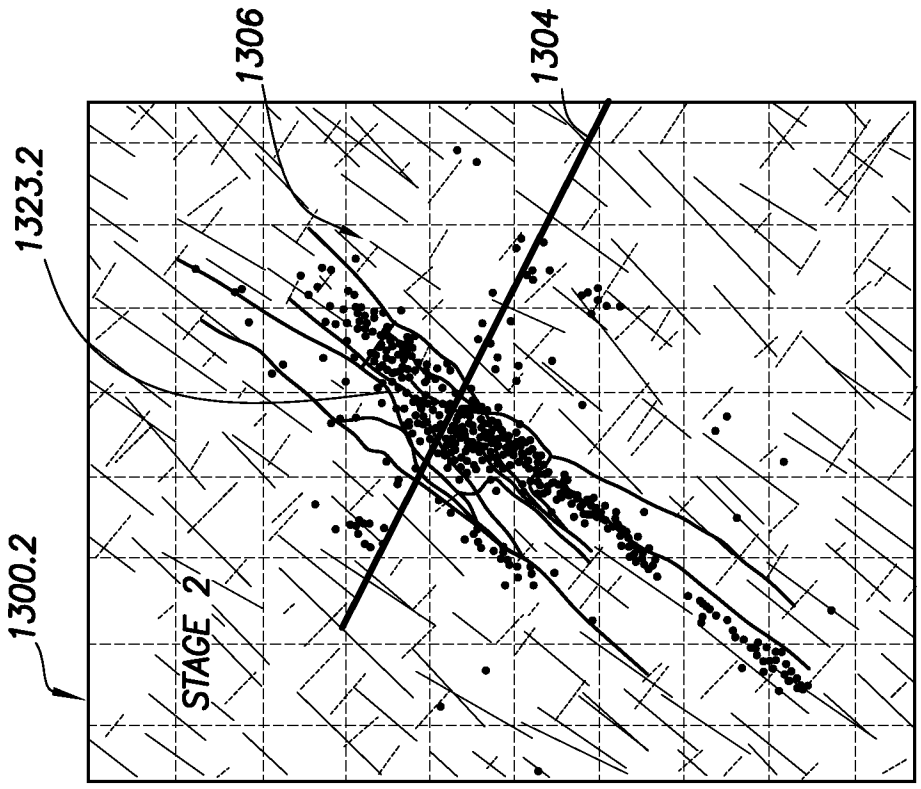

FIG.13.2

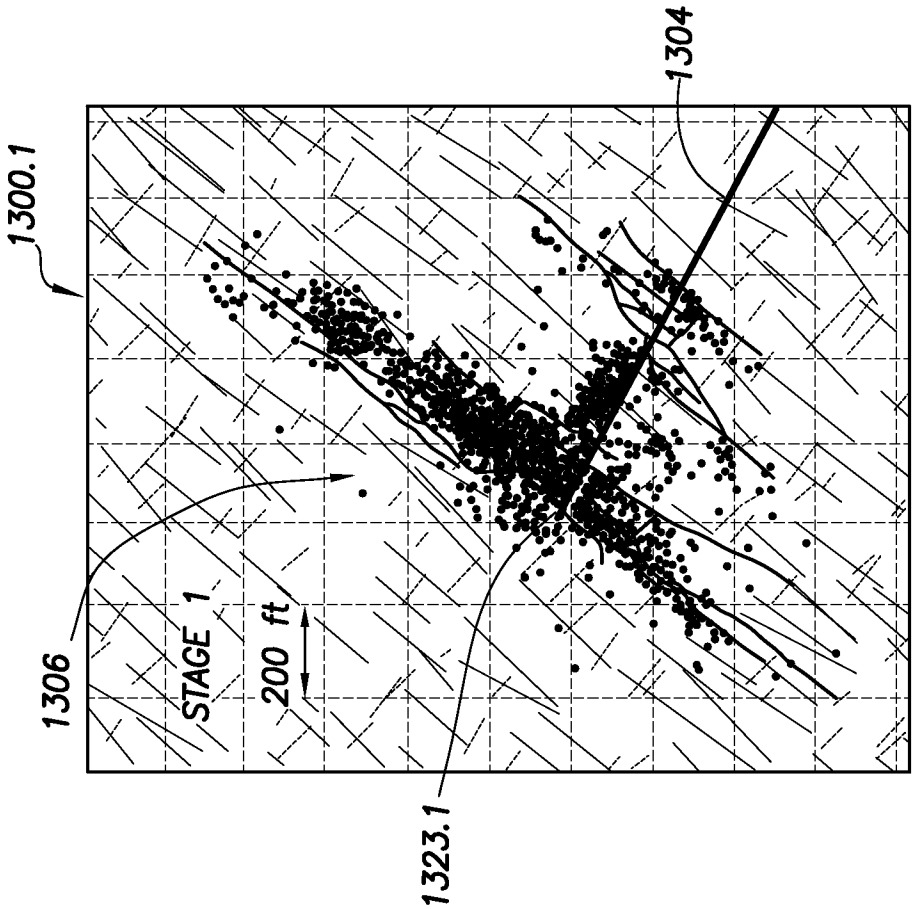

FIG.13.1

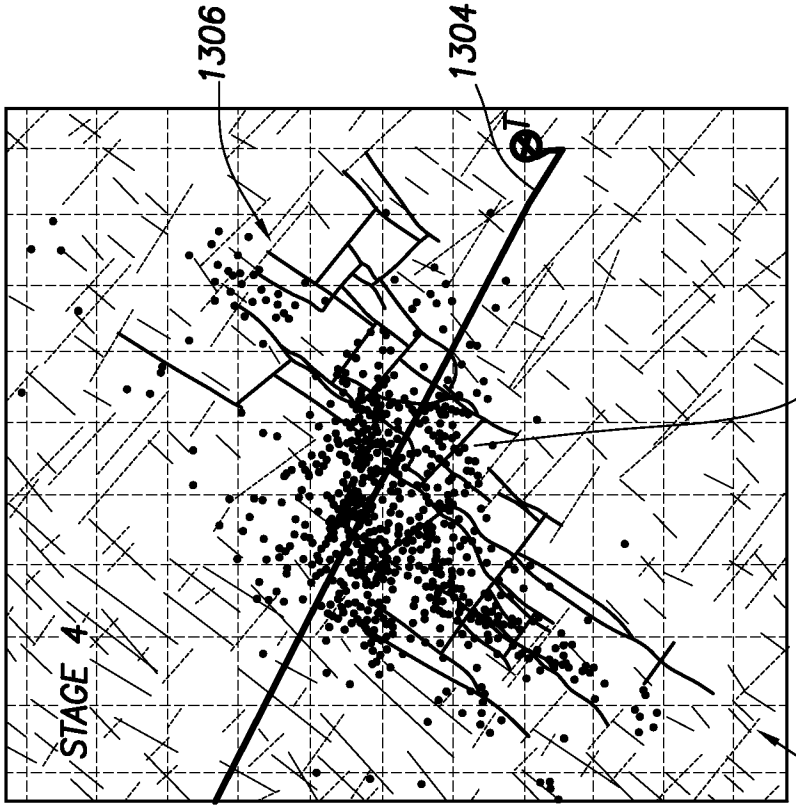

FIG. 13.4

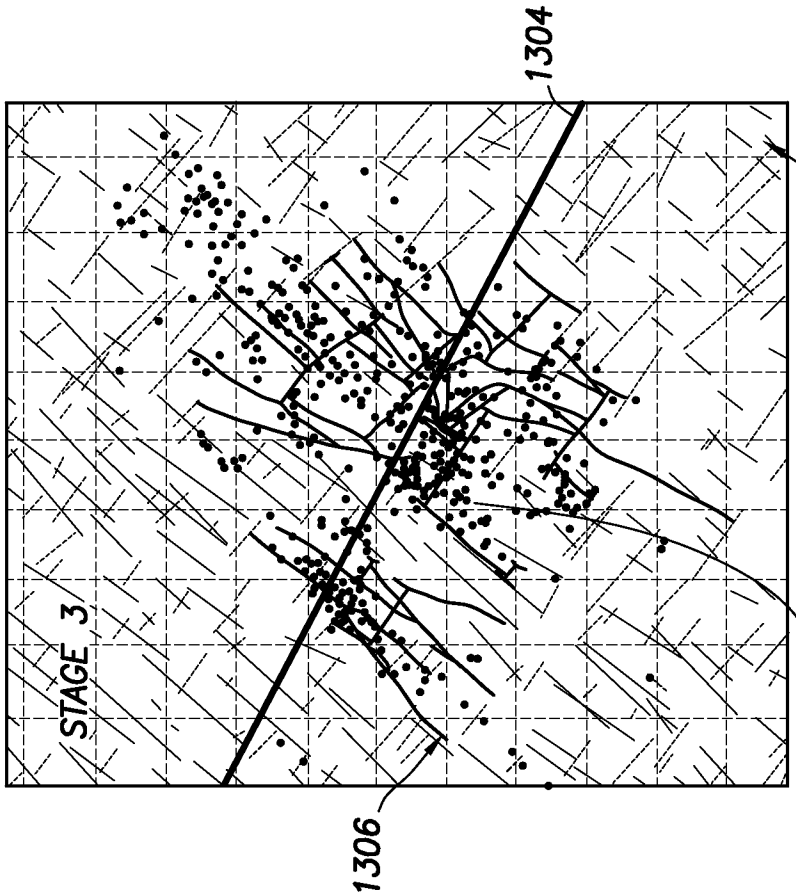

FIG. 13.3

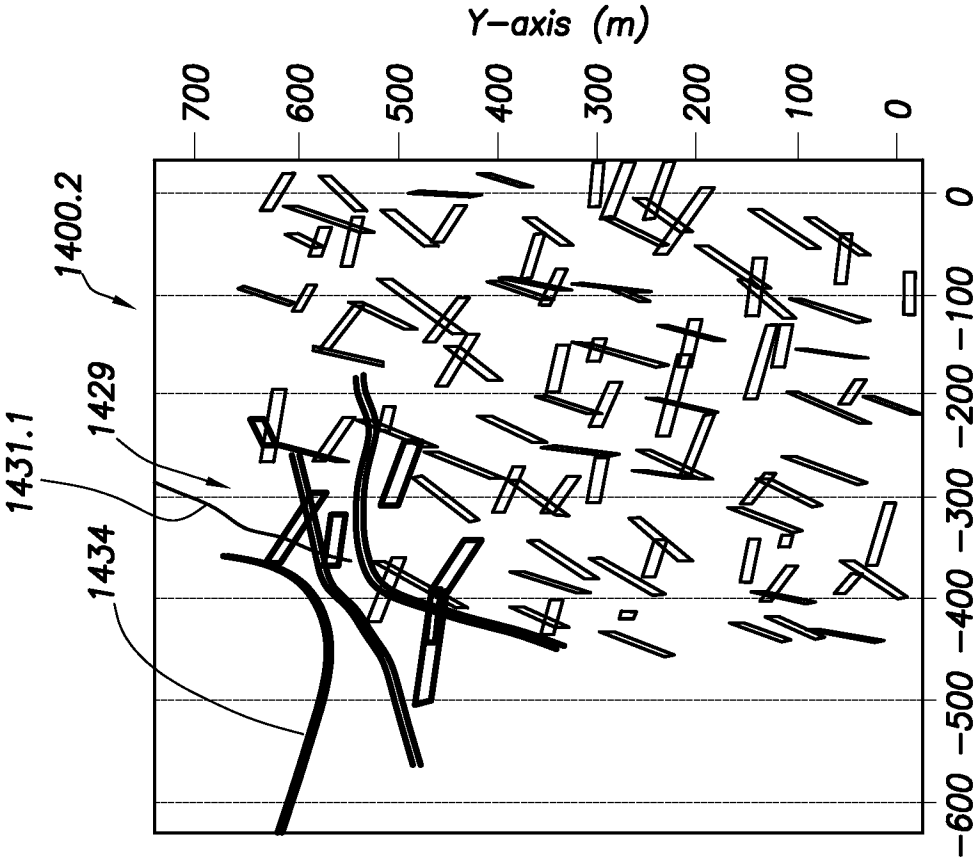

FIG.14.2

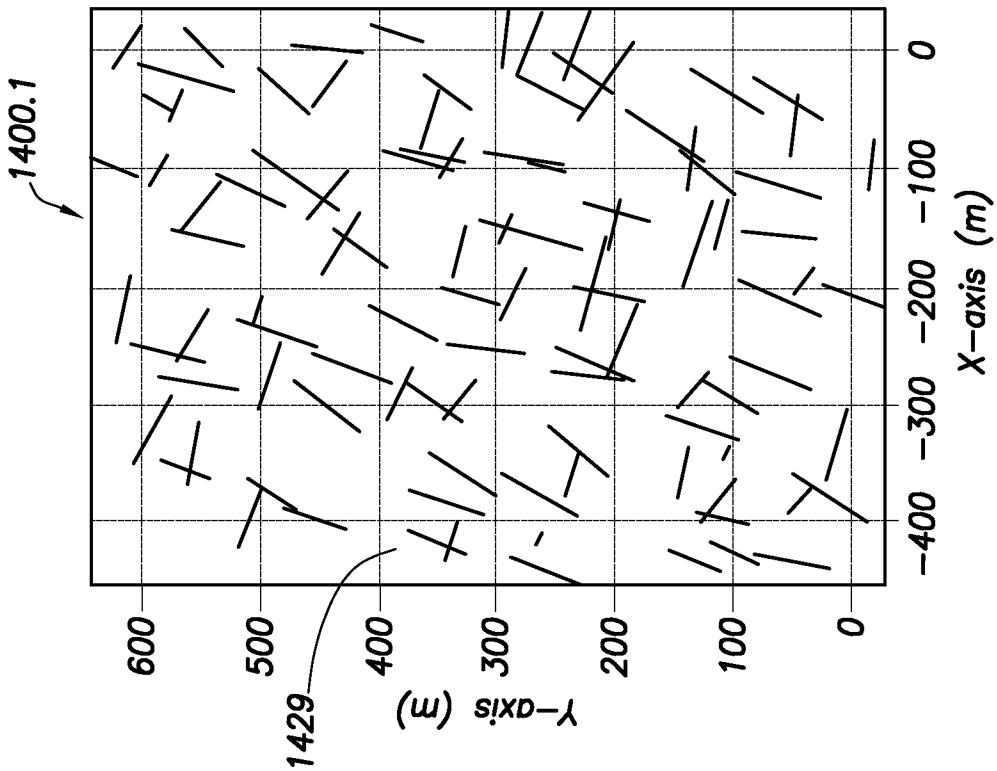

FIG.14.1

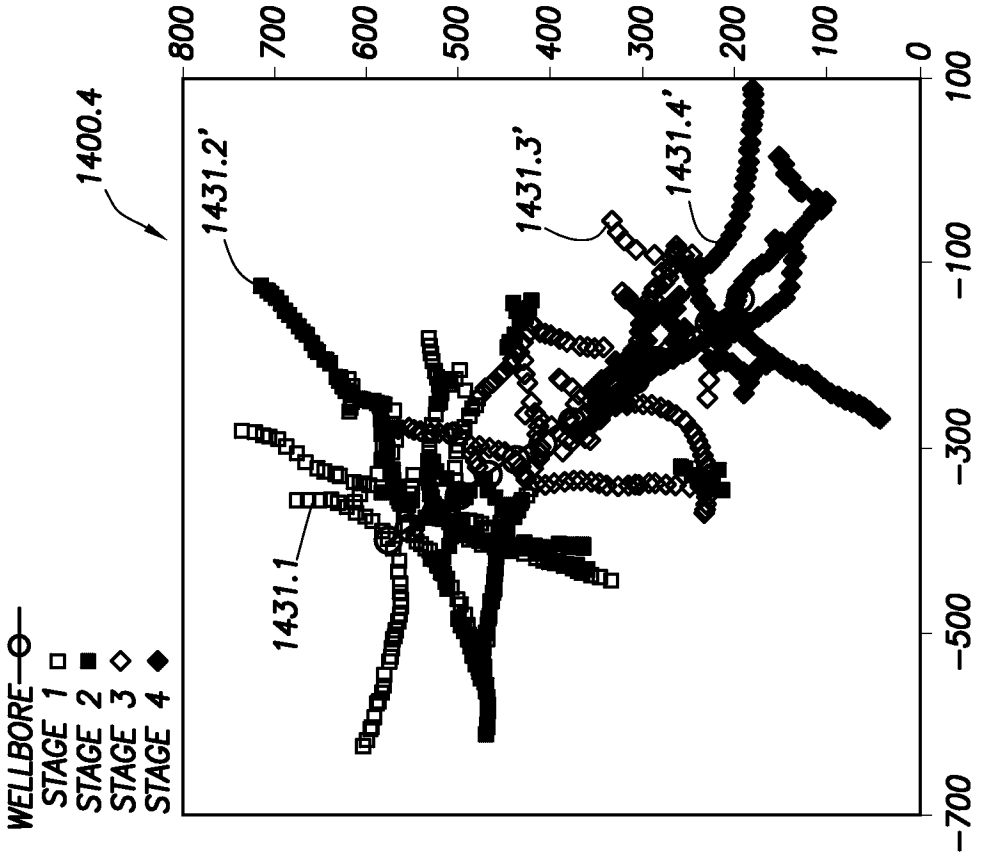

FIG.14.4

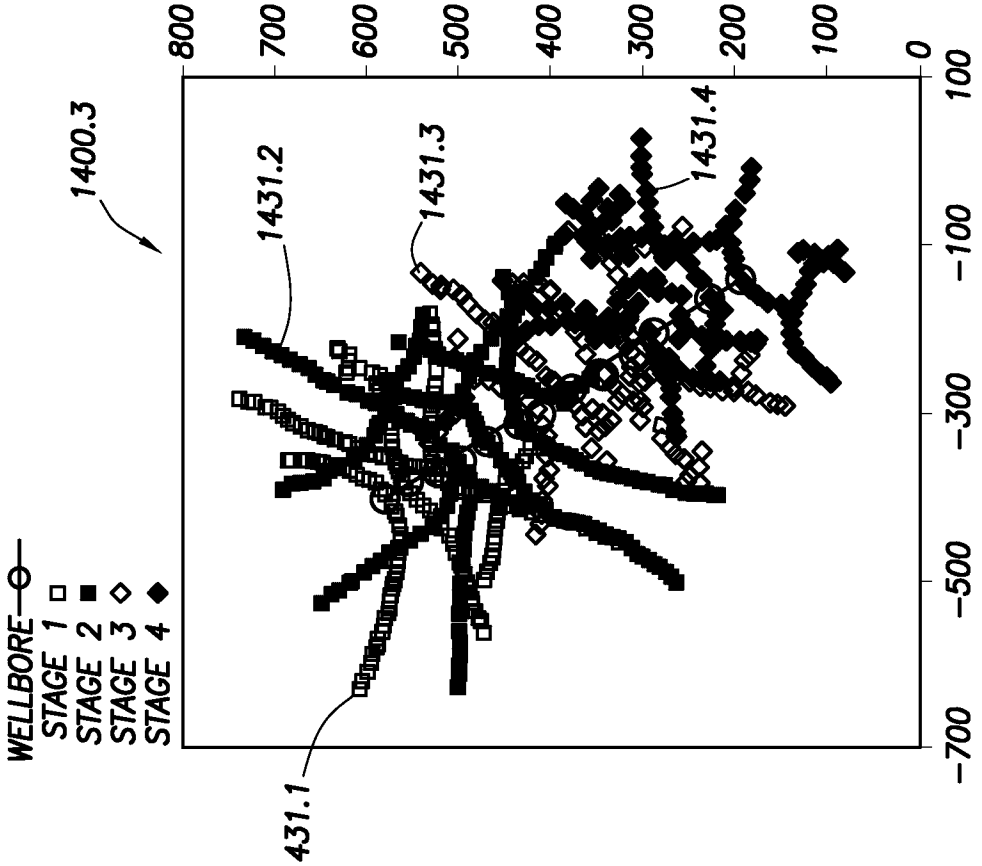

FIG.14.3

FIG. 15

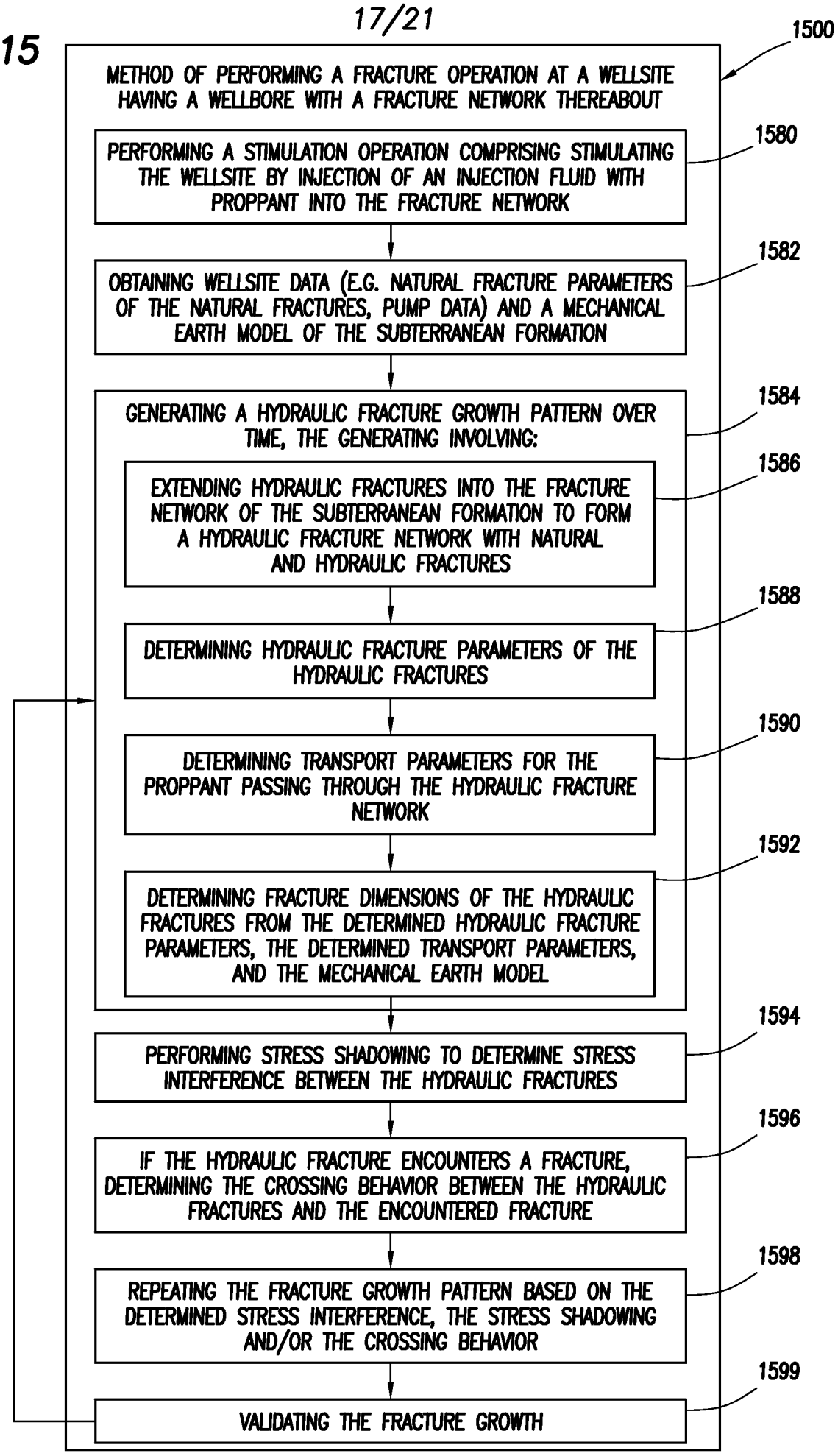
1500
METHOD OF PERFORMING A FRACTURE OPERATION AT A WELLSITE HAVING A WELLBORE WITH A FRACTURE NETWORK THEREABOUT
1580
PERFORMING A STIMULATION OPERATION COMPRISING STIMULATING THE WELLSITE BY INJECTION OF AN INJECTION FLUID WITH PROPPANT INTO THE FRACTURE NETWORK
1582
OBTAINING WELLSITE DATA (E.G. NATURAL FRACTURE PARAMETERS OF THE NATURAL FRACTURES, PUMP DATA) AND A MECHANICAL EARTH MODEL OF THE SUBTERRANEAN FORMATION
1584
GENERATING A HYDRAULIC FRACTURE GROWTH PATTERN OVER TIME, THE GENERATING INVOLVING:
1586
EXTENDING HYDRAULIC FRACTURES INTO THE FRACTURE NETWORK OF THE SUBTERRANEAN FORMATION TO FORM A HYDRAULIC FRACTURE NETWORK WITH NATURAL AND HYDRAULIC FRACTURES
1588
DETERMINING HYDRAULIC FRACTURE PARAMETERS OF THE HYDRAULIC FRACTURES
1590
DETERMINING TRANSPORT PARAMETERS FOR THE PROPPANT PASSING THROUGH THE HYDRAULIC FRACTURE NETWORK
1592
DETERMINING FRACTURE DIMENSIONS OF THE HYDRAULIC FRACTURES FROM THE DETERMINED HYDRAULIC FRACTURE PARAMETERS, THE DETERMINED TRANSPORT PARAMETERS, AND THE MECHANICAL EARTH MODEL
1594
PERFORMING STRESS SHADOWING TO DETERMINE STRESS INTERFERENCE BETWEEN THE HYDRAULIC FRACTURES
1596
IF THE HYDRAULIC FRACTURE ENCOUNTERS A FRACTURE, DETERMINING THE CROSSING BEHAVIOR BETWEEN THE HYDRAULIC FRACTURES AND THE ENCOUNTERED FRACTURE
1598
REPEATING THE FRACTURE GROWTH PATTERN BASED ON THE DETERMINED STRESS INTERFERENCE, THE STRESS SHADOWING AND/OR THE CROSSING BEHAVIOR
1599
VALIDATING THE FRACTURE GROWTH

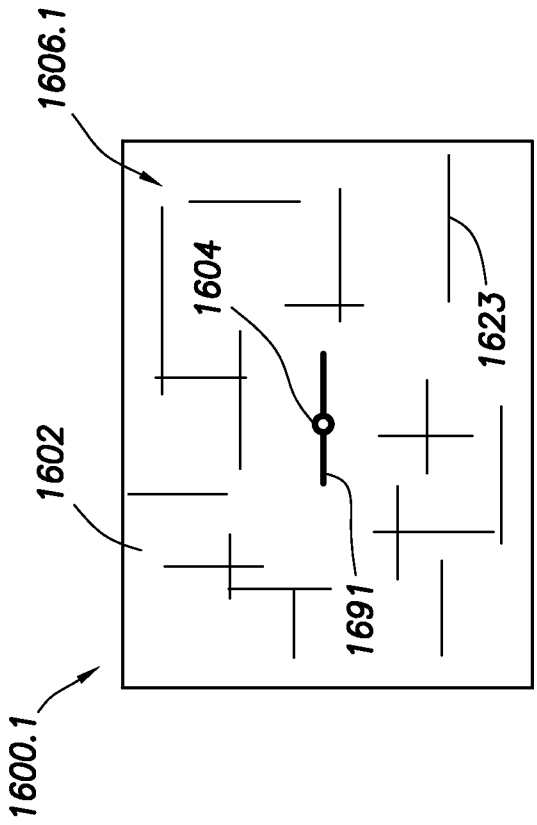

FIG.16.1

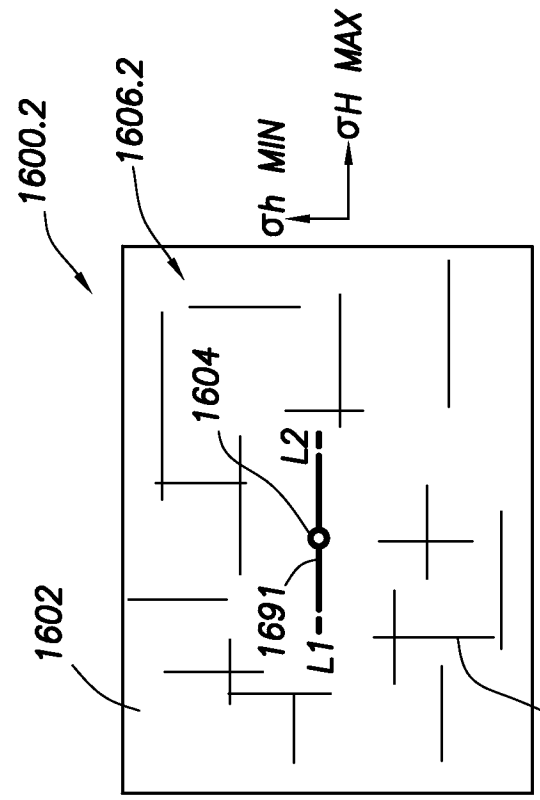

FIG.16.2

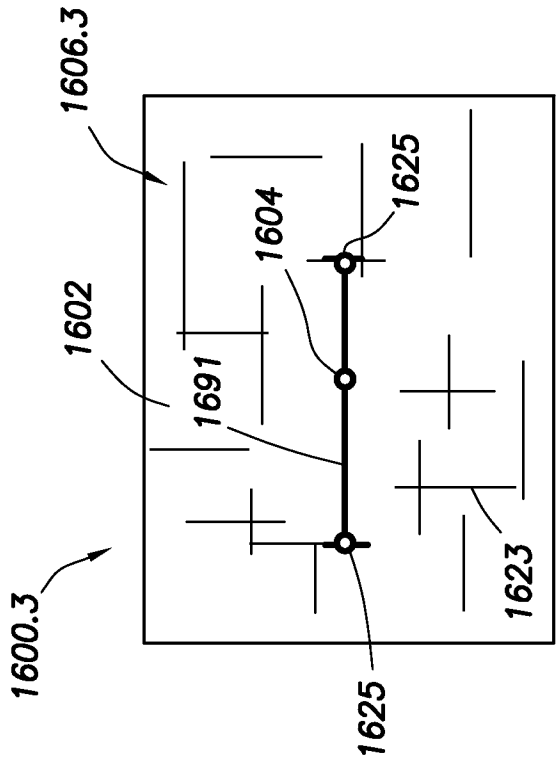

FIG.16.3

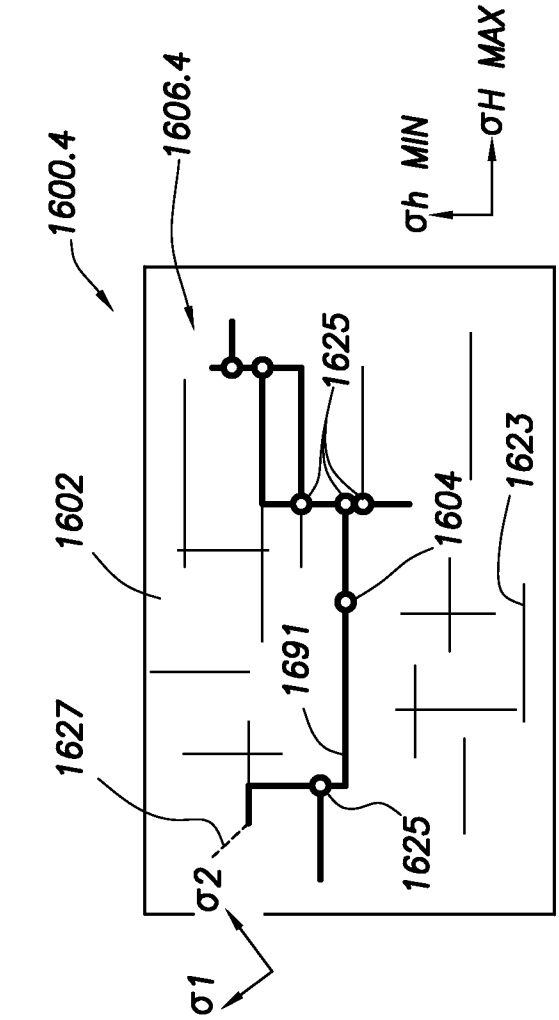

FIG.16.4

FIG. 17

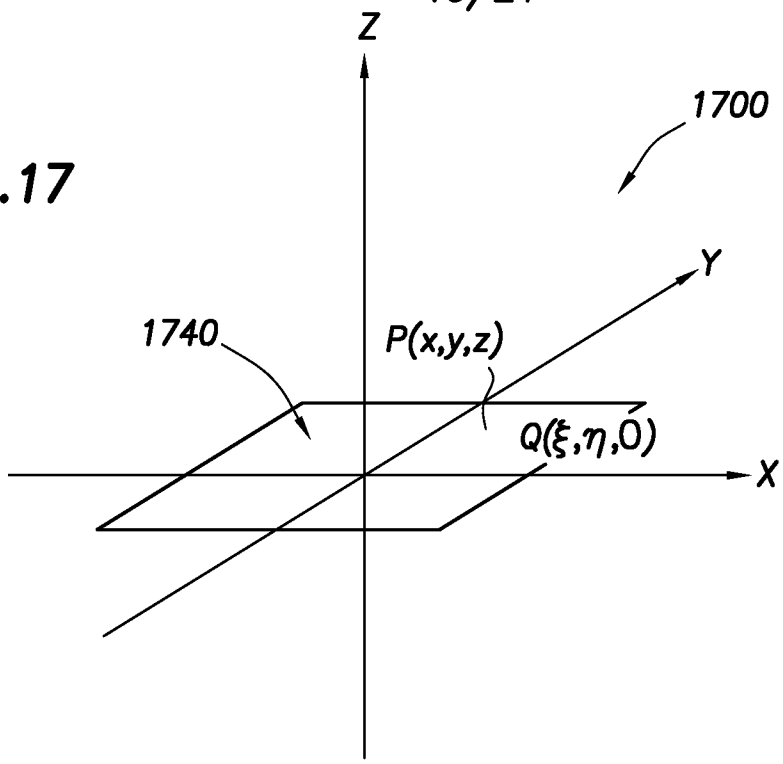
Z
1700
Y
1740
P(x,y,z)
Q(ξ,η,0)
X

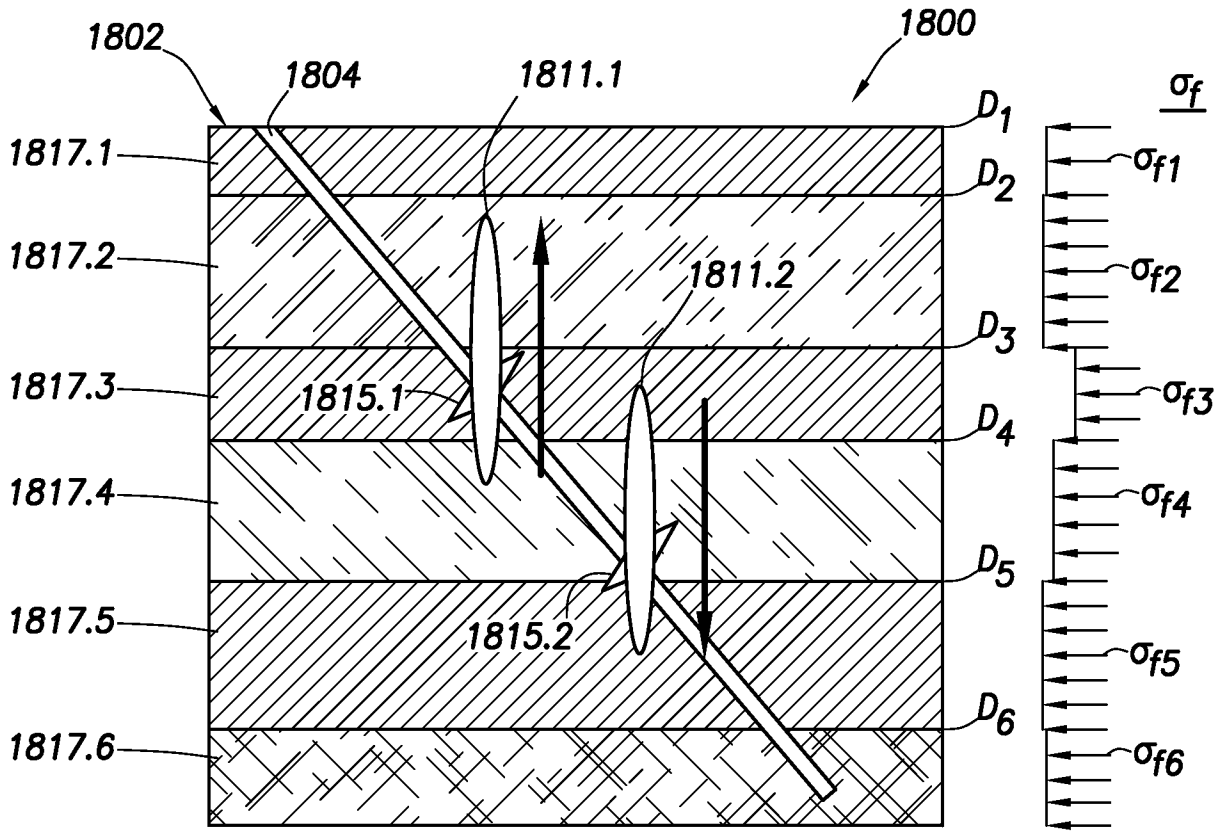
1802
1804
1811.1
1800
σ_f
1817.1
1817.2
1817.3
1817.4
1817.5
1817.6
D_1
D_2
D_3
D_4
D_5
D_6
1811.2
1815.1
1815.2
σ_{f1}
σ_{f2}
σ_{f3}
σ_{f4}
σ_{f5}
σ_{f6}

FIG. 18

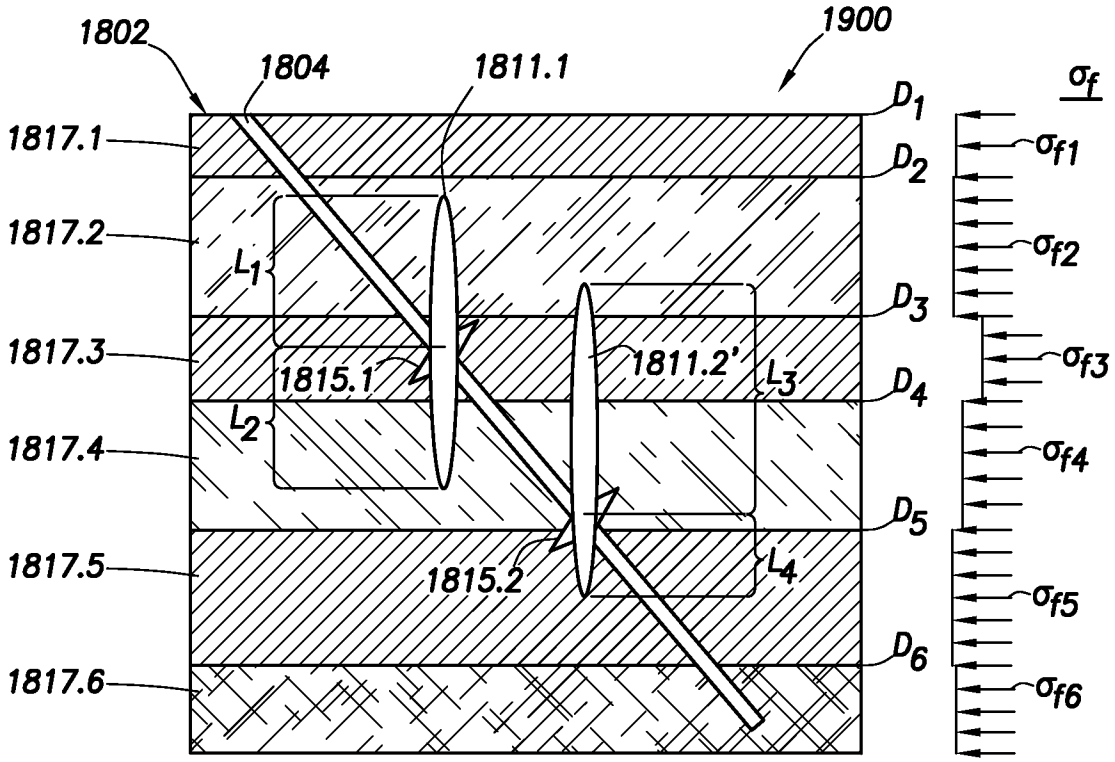
1802
1804
1811.1
1900
1817.1
1817.2
1817.3
1817.4
1817.5
1817.6
L_1
L_2
1815.1
1811.2'
L_3
L_4
1815.2
D_1
D_2
D_3
D_4
D_5
D_6
σ_f
σ_{f1}
σ_{f2}
σ_{f3}
σ_{f4}
σ_{f5}
σ_{f6}

FIG. 19

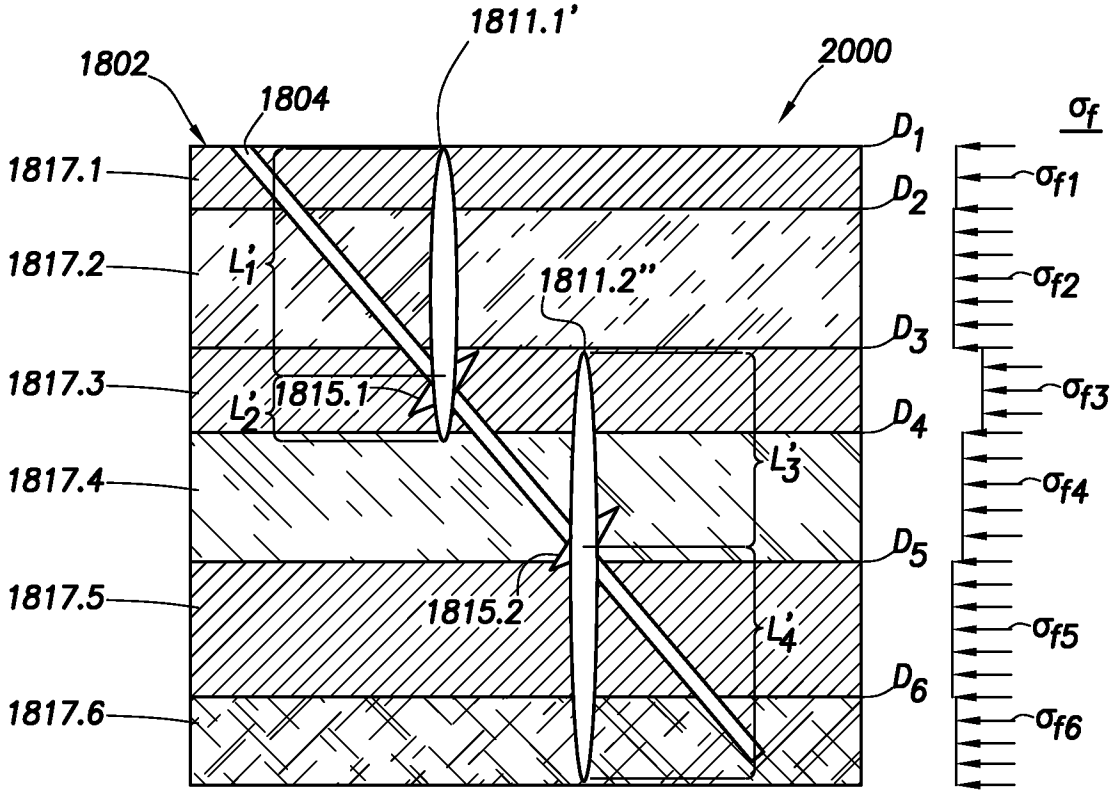
1811.1'
2000
1802
1804
1817.1
1817.2
1817.3
1817.4
1817.5
1817.6
L_1'
L_2'
1811.2"
1815.1
L_3'
L_4'
1815.2
D_1
D_2
D_3
D_4
D_5
D_6
σ_f
σ_{f1}
σ_{f2}
σ_{f3}
σ_{f4}
σ_{f5}
σ_{f6}

FIG. 20

FIG.21

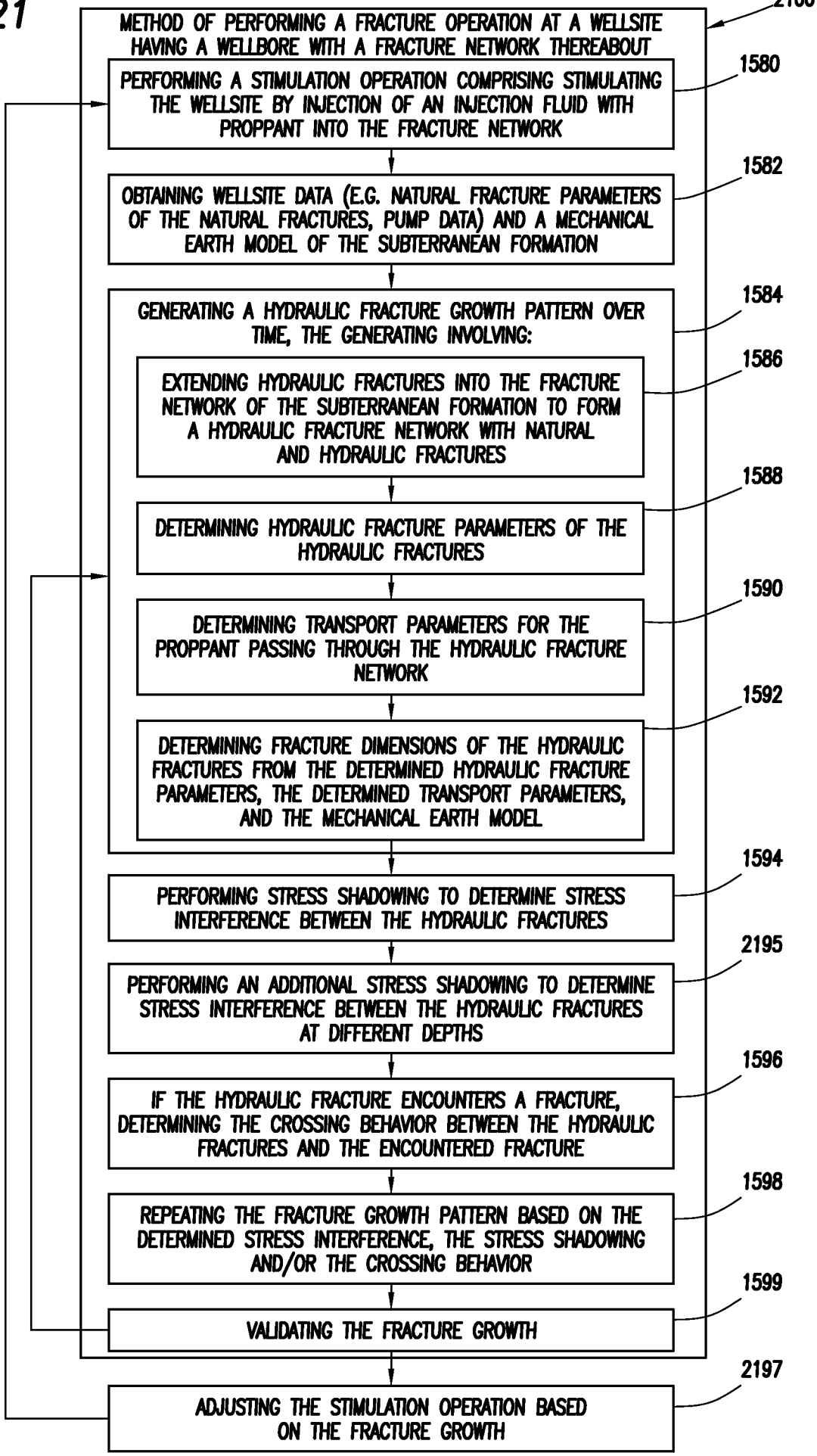
2100
METHOD OF PERFORMING A FRACTURE OPERATION AT A WELLSITE HAVING A WELLBORE WITH A FRACTURE NETWORK THEREABOUT
1580
PERFORMING A STIMULATION OPERATION COMPRISING STIMULATING THE WELLSITE BY INJECTION OF AN INJECTION FLUID WITH PROPPANT INTO THE FRACTURE NETWORK
1582
OBTAINING WELLSITE DATA (E.G. NATURAL FRACTURE PARAMETERS OF THE NATURAL FRACTURES, PUMP DATA) AND A MECHANICAL EARTH MODEL OF THE SUBTERRANEAN FORMATION
1584
GENERATING A HYDRAULIC FRACTURE GROWTH PATTERN OVER TIME, THE GENERATING INVOLVING:
1586
EXTENDING HYDRAULIC FRACTURES INTO THE FRACTURE NETWORK OF THE SUBTERRANEAN FORMATION TO FORM A HYDRAULIC FRACTURE NETWORK WITH NATURAL AND HYDRAULIC FRACTURES
1588
DETERMINING HYDRAULIC FRACTURE PARAMETERS OF THE HYDRAULIC FRACTURES
1590
DETERMINING TRANSPORT PARAMETERS FOR THE PROPPANT PASSING THROUGH THE HYDRAULIC FRACTURE NETWORK
1592
DETERMINING FRACTURE DIMENSIONS OF THE HYDRAULIC FRACTURES FROM THE DETERMINED HYDRAULIC FRACTURE PARAMETERS, THE DETERMINED TRANSPORT PARAMETERS, AND THE MECHANICAL EARTH MODEL
1594
PERFORMING STRESS SHADOWING TO DETERMINE STRESS INTERFERENCE BETWEEN THE HYDRAULIC FRACTURES
2195
PERFORMING AN ADDITIONAL STRESS SHADOWING TO DETERMINE STRESS INTERFERENCE BETWEEN THE HYDRAULIC FRACTURES AT DIFFERENT DEPTHS
1596
IF THE HYDRAULIC FRACTURE ENCOUNTERS A FRACTURE, DETERMINING THE CROSSING BEHAVIOR BETWEEN THE HYDRAULIC FRACTURES AND THE ENCOUNTERED FRACTURE
1598
REPEATING THE FRACTURE GROWTH PATTERN BASED ON THE DETERMINED STRESS INTERFERENCE, THE STRESS SHADOWING AND/OR THE CROSSING BEHAVIOR
1599
VALIDATING THE FRACTURE GROWTH
2197
ADJUSTING THE STIMULATION OPERATION BASED ON THE FRACTURE GROWTH

INTERNATIONAL SEARCH REPORT

International application No.
PCT/US2014/064205

A. CLASSIFICATION OF SUBJECT MATTER

E21B 43/26(2006.01)i, E21B 43/247(2006.01)i

According to International Patent Classification (IPC) or to both national classification and IPC

B. FIELDS SEARCHED

Minimum documentation searched (classification system followed by classification symbols)
E21B 43/26; G06F 19/00; G06G 7/48; G06F 17/18; E21B 49/00; C09K 8/62; G06G 7/00; G06F 17/40; E21B 43/247

Documentation searched other than minimum documentation to the extent that such documents are included in the fields searched
Korean utility models and applications for utility models
Japanese utility models and applications for utility models

Electronic data base consulted during the international search (name of data base and, where practicable, search terms used)
eKOMPASS(KIPO internal) & Keywords: subterranean, fracture network, proppant, natural fracture, growth pattern, earth model, fracture dimension, and stress shadowing

C. DOCUMENTS CONSIDERED TO BE RELEVANT

Category*	Citation of document, with indication, where appropriate, of the relevant passages	Relevant to claim No.
A	US 2013-0140031 A1 (COHEN et al.) 06 June 2013 See paragraphs [0062]-[0080],[0122]-[0138],[0142],[0148] and figures 14-15.	1-24
A	US 2007-0294034 A1 (BRATTON et al.) 20 December 2007 See paragraphs [0033]-[0046],[0075]-[0091],[0100]-[0107],[0132] and figure 4.	1-24
A	US 2008-0183451 A1 (WENG et al.) 31 July 2008 See paragraphs [0019]-[0024] and figure 2.	1-24
A	US 2011-0125471 A1 (CRAIG et al.) 26 May 2011 See paragraphs [0127]-[0140] and figures 1A-2C,6A-6B.	1-24
A	US 2007-0272407 A1 (LEHMAN et al.) 29 November 2007 See paragraphs [0056]-[0064] and figures 1-2,5.	1-24

☐ Further documents are listed in the continuation of Box C.

☒ See patent family annex.

* Special categories of cited documents:
"A" document defining the general state of the art which is not considered to be of particular relevance
"E" earlier application or patent but published on or after the international filing date
"L" document which may throw doubts on priority claim(s) or which is cited to establish the publication date of another citation or other special reason (as specified)
"O" document referring to an oral disclosure, use, exhibition or other means
"P" document published prior to the international filing date but later than the priority date claimed
"T" later document published after the international filing date or priority date and not in conflict with the application but cited to understand the principle or theory underlying the invention
"X" document of particular relevance; the claimed invention cannot be considered novel or cannot be considered to involve an inventive step when the document is taken alone
"Y" document of particular relevance; the claimed invention cannot be considered to involve an inventive step when the document is combined with one or more other such documents,such combination being obvious to a person skilled in the art
"&" document member of the same patent family

Date of the actual completion of the international search	Date of mailing of the international search report
23 February 2015 (23.02.2015)	**23 February 2015 (23.02.2015)**

Name and mailing address of the ISA/KR
International Application Division
Korean Intellectual Property Office
189 Cheongsa-ro, Seo-gu, Daejeon Metropolitan City, 302-701, Republic of Korea
Facsimile No. ++82 42 472 3473

Authorized officer
CHOI, Hyun Goo
Telephone No. +82-42-481-8288

INTERNATIONAL SEARCH REPORT

Information on patent family members

International application No.
PCT/US2014/064205

Patent document cited in search report	Publication date	Patent family member(s)	Publication date
US 2013-0140031 A1	06/06/2013	CA 2804833 A1	30/07/2013
US 2007-0294034 A1	20/12/2007	CA 2654730 A1	21/12/2007
		CA 2654730 C	28/01/2014
		EA 017421 B1	28/12/2012
		EA 200970017 A1	30/06/2009
		MX 2008015872 A	12/01/2009
		US 7953587 B2	31/05/2011
		WO 2007-147135 A2	21/12/2007
		WO 2007-147135 A3	06/03/2008
US 2008-0183451 A1	31/07/2008	CA 2676675 A1	07/08/2008
		US 2013-0066617 A1	14/03/2013
		US 2014-0136173 A1	15/05/2014
		US 8412500 B2	02/04/2013
		US 8571843 B2	29/10/2013
		WO 2008-093264 A1	07/08/2008
US 2011-0125471 A1	26/05/2011	AR 079147 A1	28/12/2011
		AU 2010-322929 A1	07/06/2012
		CA 2778313 A1	03/06/2011
		EP 2504524 A2	03/10/2012
		US 8392165 B2	05/03/2013
		WO 2011-064541 A2	03/06/2011
		WO 2011-064541 A3	15/12/2011
US 2007-0272407 A1	29/11/2007	None	